J. Embryol. exp. Morph. **89**, 175–208 (1985)
Printed in Great Britain © *The Company of Biologists Limited 1985*

Maturation and polarization of the endocytotic system in outside blastomeres during mouse preimplantation development

TOM P. FLEMING AND SUSAN J. PICKERING
Department of Anatomy, Downing Street, Cambridge, CB2 3DY, U.K.

SUMMARY

The maturation and distribution of the endocytotic apparatus in outside cells of cleavage-stage mouse embryos have been studied to determine the nature and sequence of changes associated with the differentiation of the polarized trophectoderm epithelium of the blastocyst. Various quantitative and qualitative techniques used at the light and electron microscopic levels have revealed an incremental pattern of endocytotic maturation and polarization. Oocytes, eggs and blastomeres within embryos up to the early 8-cell stage contain clusters of prelysosomal endocytotic vesicles (endosomes) distributed randomly in the cortical cytoplasm. During the 8-cell stage and continuing into the early 16-cell stage, endosomes become progressively localized in the apical cytoplasm beneath the microvillous pole. Endosome polarization is initiated prior to overt polarization of the surface membrane. Concomitant with endosome polarization, pinocytotic activity at the cell surface, revealed by horseradish peroxidase labelling, becomes segregated preferentially to the apical rather than the basolateral membrane. The final maturation phase occurs at the late 16-cell stage when secondary lysosomes, characterized by trimetaphosphatase reactivity, form and polarize in the basal cytoplasm.

INTRODUCTION

A major differentiative feature of mouse preimplantation development is the generation, by the blastocyst stage, of a mature, polarized, outer epithelium, the trophectoderm (TE). TE cell polarity is most clearly shown by the presence of junctional complexes, including zonular tight junctions, at the apicolateral margins of apposed cells (Ducibella, Albertini, Anderson & Biggers, 1975; Magnuson, Demsey & Stackpole, 1977) which permit vectorial fluid transport during cavitation and maintain the asymmetry of apical and basolateral membrane compartments. These membrane domains differ in their structure (Calarco & Epstein, 1973; Nadijcka & Hillman, 1974; Johnson & Ziomek, 1982), antigenic properties (Searle & Jenkinson, 1978; Wiley & Eglitis, 1981; Randle, 1982), enzyme constituents (Borland, 1977; Mulnard & Huygens, 1978; Izquierdo, Lopez & Marticorena, 1980; Izquierdo & Ebensperger, 1982; Kaye *et al.* 1982) and in their relative adhesiveness (Burgoyne & Ducibella, 1977; Kimber, Surani & Barton, 1982) (see also review by Johnson, 1981). Intracellular polarity within the TE is also evident with respect to organelle distribution; mitochondria and

Key words: mouse embryos, endocytosis, endosomes, lysosomes, cell polarity, ultrastructure.

cytoplasmic droplets tend to localize close to the basolateral membrane (Wiley & Eglitis, 1981) while secondary lysosomes occur preferentially in the basal cytoplasm (Fleming, Warren, Chisholm & Johnson, 1984). A corresponding cytoplasmic heterogeneity has not been detected within the inner cell mass cells (ICM) of the blastocyst and thus the possession of a polarized phenotype is a characteristic feature of TE.

A *stable* asymmetry of cellular organization is first evident in 8-cell blastomeres developing during the process of compaction, although regionalization of membrane-associated enzymes (Izquierdo *et al.* 1980; Izquierdo & Ebensperger, 1982) and of cholesterol organization (Pratt, 1985) has been reported for earlier stages. The polarization of blastomeres at the 8-cell stage is pervasive and involves the redistribution of membrane, cytoskeletal and organelle components. Thus microvilli become localized apically (Ducibella, Ukena, Karnovsky & Anderson, 1977; Handyside, 1980; Reeve & Ziomek, 1981), while focal tight junctions (Ducibella & Anderson, 1975; Magnuson *et al.* 1977) and functional gap junctions (Lo & Gilula, 1979; Goodall & Johnson, 1982, 1984; McLachlin, Caveney & Kidder, 1983) form at apposed cell surfaces. These structural asymmetries in membrane domains overlie differences in their organization at the molecular level (Pratt, 1985). A corresponding asymmetry within the cytoplasm is evident for endocytotic vesicles (Reeve, 1981*a*) and cytoskeletal actin (Johnson & Maro, 1984) which polarize apically, while the nucleus occupies a basal position (Reeve & Kelly, 1983). Changes in the distribution of other cellular components including clathrin and various membrane organelles during the 8- and 16-cell stage have been reported by Maro, Johnson, Pickering & Louvard (1985).

The heterogeneity in the cell surface at the 8-cell stage is maintained during division to the 16-cell stage leading to the formation of polar outside and apolar inside cell populations (Johnson & Ziomek, 1981; Reeve, 1981*b*). The polar and apolar phenotypes thus derived, although retaining a regulative capacity (Ziomek, Johnson & Handyside, 1982; Johnson & Ziomek, 1983), tend to divide conservatively to yield TE and ICM cell types respectively at the blastocyst stage (Ziomek & Johnson, 1982). Thus the process of polarization which occurs over two cell cycles occupies a central role in the generation of cell diversity and the establishment of a functional epithelium (reviewed Johnson, 1985*a*,*b*).

In the present paper, the process of TE epithelial development in outside blastomeres is considered in relation to the endocytotic system. Both the structural and molecular heterogeneity within the membrane of a cell in a fully differentiated epithelium and the tendency for internalization of specific molecules to occur from a particular (usually apical) domain (reviewed by Reggio, Coudrier & Louvard, 1982; Rindler, Ivanov, Rodriguez-Boulan & Sabatini, 1982; Sabatini *et al.* 1983; Herzog, 1984) necessitate a certain rigidity in the spatial organization of the endocytotic system. Such an intracellular 'response' to membrane asymmetry is essential both for an efficient processing of extracellular material and, more importantly, to control against potential randomization of surface domains by vectorial membrane traffic (Rodewald & Abrahamson, 1982). It is therefore of

interest to establish when such an endocytotic organization becomes established within the mouse early embryo and to determine the time at which endocytotic activity becomes preferentially segregated to the absorptive membrane domain.

Using conventional, quantitative, cytochemical and tracer techniques at the ultrastructural level, we provide evidence that from the 8-cell stage there are incremental advances in the maturation and polarization of the endocytotic apparatus that relate directly to the generation of TE epithelium. These events include the apical polarization of prelysosomal endosomes (endocytotic organelles of Reeve, 1981*a*,*b*) at the 8-cell stage, the formation and basal polarization of secondary lysosomes at the 16-cell stage and a progressive increase in apical membrane pinocytotic activity during the period from compaction to cavitation.

MATERIALS AND METHODS

Oocyte and embryo collection and staging

For collection of fertilized eggs and of cleavage- and cavitation-stage embryos, female HC-CFLP (Hacking & Churchill Ltd) or MF1 (Olac Ltd) mice were superovulated (5 i.u. PMS followed 45–48 h later by 5 i.u. hCG, Intervet) and mated overnight with HC-CFLP males; a vaginal plug indicated successful mating. Superovulated, unmated mice were used for collection of unfertilized oocytes. Preovulatory oocytes were obtained (a) 48 h post-PMS without hCG injection (germinal vesicle stage) or (b) 6 h post-hCG injection (first metaphase stage; Edwards & Gates, 1959) by piercing individual follicles during ovary dissection.

Recovered oocytes, eggs and embryos were transferred to HEPES-buffered Medium 2+4 mg ml^{-1} bovine serum albumin (M2+BSA; Fulton & Whittingham, 1978) and cultured where appropriate in Medium 16+4 mg ml^{-1} BSA (M16+BSA; Whittingham, 1971) under oil in Falcon dishes at 37 °C and 5 % CO_2 in air.

Fertilized eggs and unfertilized oocytes were recovered at 15 h post-hCG and, in the case of presumptive fertilized eggs, cultured in M16+BSA until 20 h post-hCG and examined for the presence of two pronuclei. Two-cell, 4-cell and precompact 8-cell embryos were obtained by flushing oviducts at the late 2-cell stage (47–50 h post-hCG) and cultured in M16+BSA until the required developmental age (4-cell, 50–58 h post-hCG; 8-cell 60–70 h post-hCG). In some instances, early 2-cell embryos were recovered at 37 h post-hCG.

In experiments where more precise timing of early 8-cell embryos was required, a stock culture of embryos containing four to seven cells was examined at hourly intervals and those embryos that had formed 8-cells since the previous inspection were picked off, cultured separately, and designated 0 h 8-cell embryos. Compacted 8-cell embryos were obtained in a similar manner by hourly inspection of stock embryos. Those which had compacted during the previous hour were pooled and designated 0 h compacted 8-cell embryos. The number of inspection periods for a given stock of embryos was restricted to avoid inclusion of abnormal or slow developing embryos in subsequent experiments. Thus 0 h compacted embryos were aged between 5–9 h from the beginning of the cell cycle.

Embryos at different ages throughout the 16- and 32-cell morula stages were likewise timed from compaction. However, in these experiments, embryos were recovered at the early 8-cell stage (60–63 h post-hCG) with any early compacted embryos removed prior to culturing. 0 h compacted embryos thus derived were cultured for varying times until required. Blastocysts were obtained by culturing morulae recovered from oviducts at 65–72 h post-hCG; for some experiments blastocysts were staged from the onset of cavitation (Chisholm *et al.* 1985).

Embryo manipulation and labelling

Removal of the zona pellucida was achieved by brief exposure (15–20 s) to prewarmed acid Tyrode's solution containing 4 mg ml^{-1} polyvinylpyrrolidone (Nicolson, Yanagimachi & Yanagimachi, 1975) followed by extensive washing in M2+BSA.

Embryo decompaction was carried out by incubation in Ca^{2+}-free M2 or M16+6 mg ml^{-1} BSA for 10–15 min at 37°C.

Routine labelling of endocytotic organelles was achieved by incubation for the specified time in M16+BSA containing 5 mg ml^{-1} horseradish peroxidase (HRP; Sigma Type II) at 37°C. Prolonged HRP incubation does not appear to have any detrimental effect on subsequent development (blastocyst formation, blastocyst and ICM cell number, potential to form outgrowths) according to Reeve (1981*a*).

Endocytotic labelling experiments on isolated cells

Late 4-cell (55–60 h post-hCG) and compacted 8-cell embryos were freed from their zonae, and disaggregated to single blastomeres using a flame-polished micropipette following incubation in Ca^{2+}-free medium. Small groups (four or five) of 1/4 or 1/8 cells thus derived were transferred into drops of HRP-containing M16+BSA with the cells spaced apart, and returned to culture. At hourly intervals, 1/4 or 1/8 cell stocks were examined for division to 2/8 or 2/16 couplets respectively. Divided cells from each inspection were collected, designated 0 h 2/8 or 2/16 couplets, and cultured as individual pairs for varying periods in microdrops of M16+BSA with or without HRP (see below) in Sterilin dishes; for 2/16 couplets, Ca^{2+}-free medium was used. 0 h 2/8 couplets were cultured for varying periods between 0 and 8 h whilst 2/16 pairs were cultured for between 0 and 12 h. When the culture period was for 6 h or less, couplets were maintained throughout in M16+BSA; pairs cultured for longer periods were initially placed in HRP-containing medium and transferred to M16+BSA for the terminal 6 h.

At the end of the culture period, pairs were labelled by indirect immunofluorescence for evidence of surface polarity using heat-inactivated rabbit anti-mouse species antiserum (RAMS) diluted 1:15 in M2+BSA for 10 min, washed three times in M2+BSA and incubated in fluorescein-conjugated goat anti-rabbit IgG (FITC-GAR; Miles Labs) diluted 1:15 in M2+BSA for 10 min. Couplets were subsequently washed again in M2+BSA and fixed for 15 min in 4% paraformaldehyde in phosphate-buffered saline, and returned to M2+BSA for temporary storage.

HRP localization was visualized using the aminoethylcarbazole (AEC) reaction (Reeve, 1981*a*,*b*). Two mg AEC (Sigma) were dissolved in 0·5 ml dimethylformamide to which was added 9·5 ml acetate buffer (pH 5·0, 50 mM). The reaction mixture was Millipore filtered and, immediately before use, one drop of freshly prepared 3% (v/v) H_2O_2 was added. Cells were stained for 20–30 min, washed in M2+BSA and transferred to wells of a tissue-typing slide (Baird & Tatlock) in drops of M2+BSA under oil.

Cells were examined for HRP localization and FITC labelling using a Zeiss Universal photomicroscope fitted with a Zeiss filter set 487709. Photomicrographs were taken with Kodak Tri-X 35 mm film.

Quantitative ultrastructural analyses

In addition to qualitative fine structural studies on the morphology and localization of endocytotic organelles within oocytes and a range of preimplantation stages, quantitative TEM analyses were also carried out on particular stages as follows.

Endosome distribution was assessed within blastomeres from zona-intact early 8-cell embryos (2 h postformation), 1 h compacted 8-cell embryos and 9 h compacted 16-cell embryos (outside blastomeres only). Large-size electron micrographs (standardized magnification ×7000; print size 23×20 cm) of cells sectioned approximately through the centre of the nucleus were used to record endosome number per unit area of apical, basal or total cytoplasm. To avoid misinterpretation, profiles of endosome-like structures smaller than 0·1 μm diameter were not included in the analysis. Apical and basal cytoplasm were separated on each print by a line drawn across the cell, through the centre of the nucleus on an axis parallel to the apical surface or, when this was convex, parallel to a line linking the apical points of intercellular contact. Cells with unusual profiles that did not conform to this method of analysis were omitted. A total of 110 cells (approximately 2 cells per embryo) was analysed; the means obtained for each embryo stage were compared using Student's t-test.

Pinocytotic activity. Estimates of the relative pinocytotic activity occurring at apical and basolateral membrane faces were obtained for the following zona-intact stages: early 8-cell (2 h postformation), 1 h compacted 8-cell, 9 h compacted 16-cell; 6 h postcavitation blastocyst. 1 h and 9 h decompacted 8- and 16-cell embryos were also analysed as controls for tracer accessibility (see below).

Embryos at each stage were incubated in M16+BSA containing HRP for 10 or 20 min at 37 °C, rapidly washed in M2+BSA (15–20 s) and fixed for electron microscopy; 8-cell stages were also incubated in HRP for 5 min. Decompacted embryos were incubated, and also subsequently washed, in calcium-free medium. Blastocysts were collapsed with a microinjection needle (tip diameter 0·5 μm) 45 min prior to HRP incubation in order to equalize tracer accessibility to both sides of the TE cells.

Unstained ultrasections taken from the midregion of embryos from each group were assessed for the number of HRP-positive pinocytotic vesicles (PVs) occurring at apical and basolateral membrane faces of outside cells. For all groups except decompacted 8- and 16-cell stages, the apical surface was defined as the outward facing region of membrane, free of cell contact. For decompacted stages, apical membrane referred to the region corresponding to the microvillous pole. Analyses were confined to blastomeres sectioned through their nucleus and, to reduce error in determining PV derivation, only those PVs occurring within 0·5 μm of the respective membrane face were scored. Data obtained for each cell profile scored were standardized to the length of the relative membrane face (excluding microvilli) derived from measurements made on large-size electron micrographs at a fixed magnification; mean values were finally expressed as an *index of pinocytosis* (IP) = PV number/10 μm apical or basolateral membrane. PV data for the *whole* cell profile were also recorded. A total of 271 cells was examined and Student's t-test was used for statistical comparisons.

Endosome labelling characteristics. Early and compacted 8-cell stages and compacted 16-cell embryos labelled with HRP for specific times prior to fixation and used in the analysis of pinocytotic activity described above were also employed to compare the extent of endosome labelling with time and embryo stage. The proportion of HRP-positive endosomes in apical, basal and total cytoplasm of suitable cell profiles was determined from electron micrographs at a standardized magnification. Apical and basal cytoplasmic zones were as defined in the endosome distribution analysis. A total of 141 cells was examined; mean values were compared using Student's t-test following arcsin transformation of percentage data (Bishop, 1966).

Lysosome cytochemistry

Three techniques were employed for the detection of lysosomal hydrolases at the ultrastructural level: acid phosphatase, aryl sulphatase and trimetaphosphatase. For each enzyme, late 2-cell, 1 h compacted 8-cell and mid-expanded blastocyst stages, both with and without zonae, were examined following glutaraldehyde fixation. For the trimetaphosphatase reaction, 12 h postcompaction 16-cell stage morulae were also processed.

The acid phosphatase reaction was carried out according to the modified Gomori procedure described by Lewis & Knight (1977) using sodium β-glycerophosphate (Sigma) as substrate. The reaction was performed both at the conventional pH 5·2 using 0·1 M-tris-maleate buffer and at pH 4·0 using 0·1 M-acetate buffer. Embryos were incubated for 1 h at 37 °C.

The protocol employed for the detection of aryl sulphatase was that of Hopsu-Havu, Arstila, Helminen & Kalimo (1967), using p-nitrocatechol sulphate (Sigma), as substrate. The reaction was carried out at pH 5·5 and pH 4·0 in acetate buffer; incubations were for 1 h at 37 °C.

Trimetaphosphatase localization was carried out according to Doty, Smith, Hand & Oliver (1977) with sodium trimetaphosphate (Sigma) used as substrate. Embryos were incubated at pH 3·9 (acetate buffer), for 1 h at 37 °C.

For each procedure, control embryos were incubated in substrate-free medium; mouse liver was used as a positive control.

Transmission electron microscopy

Embryos were routinely fixed in 3 % glutaraldehyde in 0·1 M-cacodylate buffer (pH 7·3) for 30 min at room temperature, washed twice in buffer and postfixed in similarly buffered 1 %

osmium tetroxide for 30 min. Embryos were washed subsequently in distilled water, *en bloc* stained with saturated aqueous uranyl acetate for 30 min (omitted for HRP-treated embryos), dehydrated in a graded ethanol series and embedded in Spurr's resin.

In order to label the plasma membrane, embryos (2-cell, compacted 8-cell, blastocysts) without zonae were fixed (both glutaraldehyde and osmium steps) in the presence of 0·1% ruthenium red (Sigma) according to Luft (1971).

For enzyme localization, HRP-treated embryos were incubated after glutaraldehyde fixation for 30 min at room temperature in 0·1 M Tris–HCl buffer (pH 7·3) containing 0·5 mg ml^{-1} diaminobenzidine tetrahydrochloride (DAB; Sigma) and 0·03% H_2O_2. An endogenous peroxidase activity was not detectable at the EM level in DAB-reacted embryos not incubated in HRP.

Ultrathin sections were cut on an LKB Ultrotome III, stained with alcoholic uranyl acetate and lead citrate, and viewed in an AEI 6B electron microscope at 80 kV. Unstained sections examined at 40 or 60 kV were routinely used for HRP-incubated material.

RESULTS

The morphology, composition and distribution of the endocytotic organelles and the polarity of the processing pathway were found to alter at different periods during preimplantation development. These phases in the maturation of the endocytotic system are described and, where appropriate, quantified according to the developmental stages at which they occur.

Oocyte to 4-cell stage

In germinal vesicle and first metaphase staged preovulatory oocytes (Fig. 1A), unfertilized oocytes, fertilized eggs, and cleavage stages up to the 4-cell stage (Fig. 1B), the endocytotic organelles occur as discrete vesicular clusters localized almost exclusively in the cortical cytoplasm. Clusters in early cleavage stages are generally smaller than those in oocytes and are found beneath both outward facing and apposed regions of the cell membrane (Fig. 1B). Following incubation in horseradish peroxidase (HRP), these organelles are the only intracellular structures that accumulate tracer (Fig. 1C).

Each endocytotic cluster consists of several spherical or flattened, electron-lucent vacuoles (0·1–0·5 μm diameter) with intervening smaller (70 nm), medium dense tubular or vesicular structures (TVS) which are often symmetrically arranged around the vacuoles (Fig. 2A,C). In some clusters, vesicular structures are also found *inside* the vacuolar compartment (Fig. 2B), thus explaining the classical terminology of these organelles within rat (Sotelo & Porter, 1959; Izquierdo & Vial, 1962; Schlafke & Enders, 1967; Stastna, 1974; Dvorak, 1978) and mouse (Calarco & Brown, 1969) blastomeres as multivesicular bodies. However, for consistency with the modern literature on prelysosomal endocytotic compartments (Helenius, Mellman, Wall & Hubbard, 1983), the term *endosome* will be used hereafter. In differentiated cells, these organelles represent the initial site of accumulation of internalized substances where, by virtue of their acidic yet hydrolase-free milieu, components are 'sorted' prior to further processing

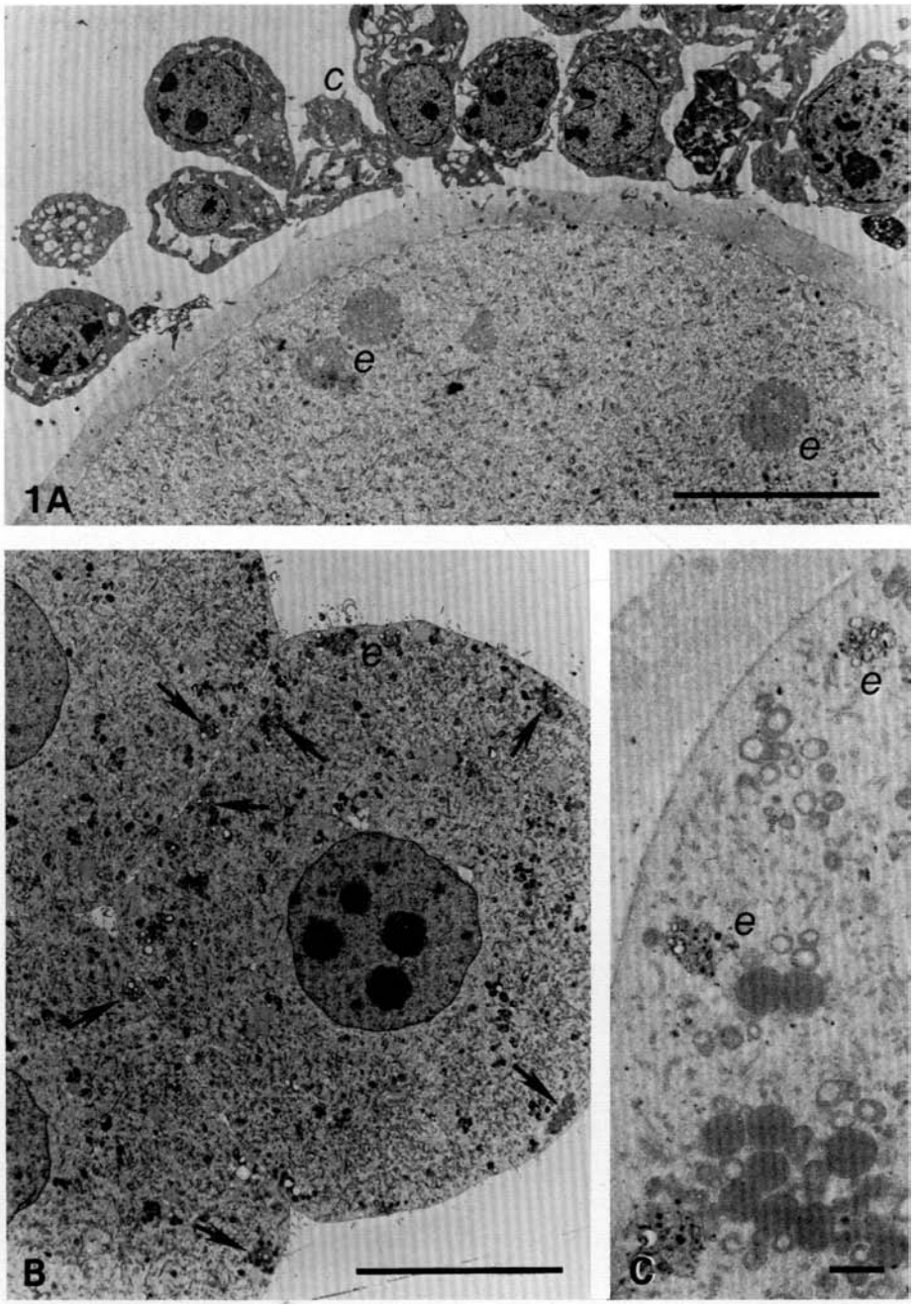

Fig. 1. Low power micrographs of endocytotic organelle distribution in early stages. (A) Cortical region of first metaphase stage oocyte with cumulus cells (*c*) attached. The oocyte cytoplasm contains spherical clusters of endocytotic vesicles (endosomes, *e*). Bar = 10 μm. (B) 4-cell embryo showing endocytotic vesicle clusters (*e*, arrows) distributed randomly in the cortical cytoplasm beneath both outward facing and apposed regions of cell membrane. Bar = 10 μm. (C) Portion of the cortical cytoplasm of a 2-cell embryo preincubated in horseradish peroxidase (HRP) for 1 h prior to fixation to label the endocytotic organelles (*e*); unstained section. Bar = 1 μm.

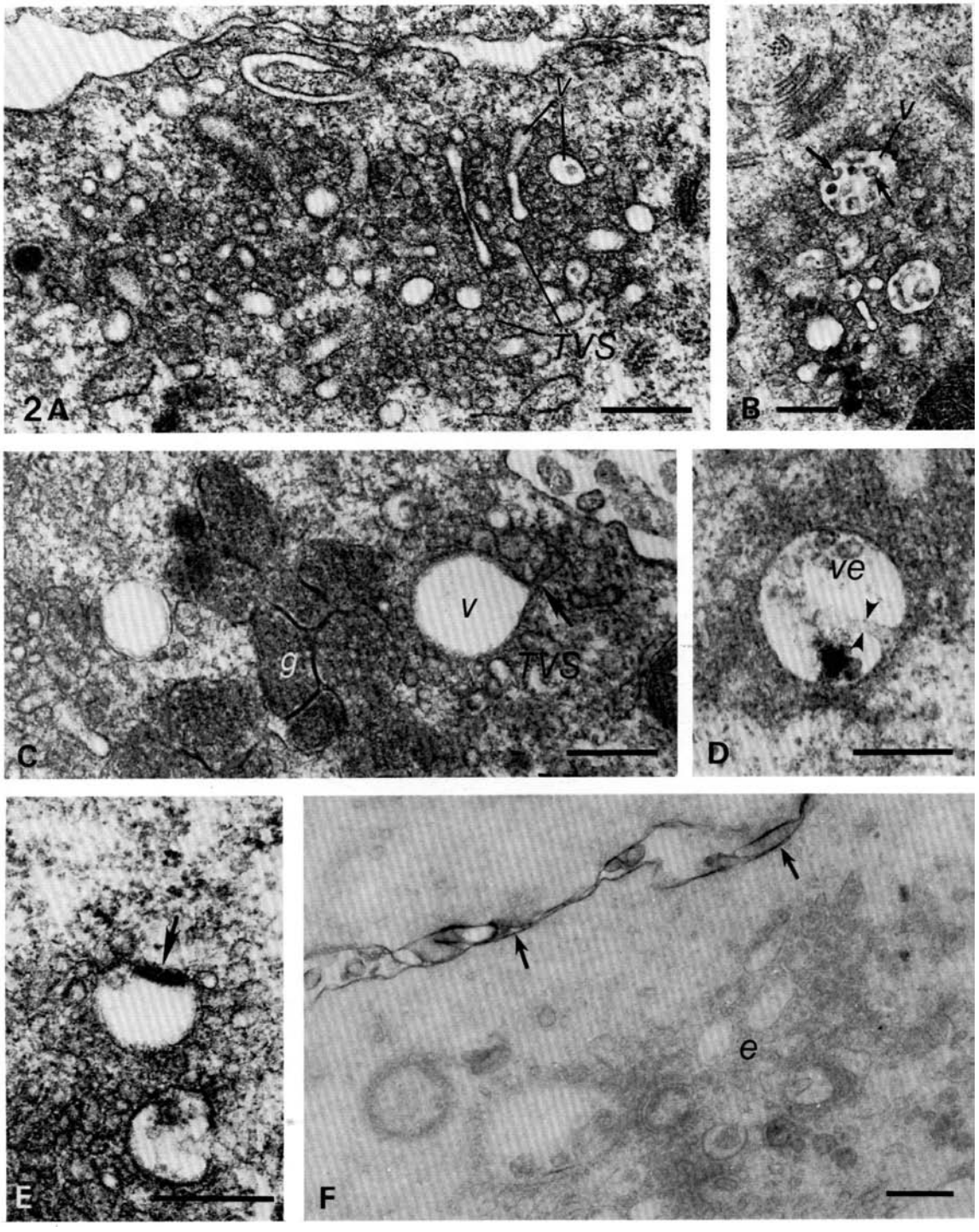
v
TVS
2A
v
B
v
g
TVS
C
ve
D
E
e
F

(Helenius *et al.* 1983). A close interrelationship between the three components of the mouse embryo endosome is evident in favourable sections where vacuole and TVS membranes are seen in continuity (Fig. 2C) and a deep invagination is found in the vacuolar membrane indicative of the formation of internalized vesicles (Fig. 2D). In a small proportion of endosome profiles, an electron-dense 'mat' is present on one region of the cytoplasmic face of the vacuole membrane which is free of TVS elements (Fig. 2E).

When 2-cell embryos were fixed in the presence of ruthenium red as a marker for cell membrane, endosome clusters were consistently unlabelled (Fig. 2F) and therefore represent true intracellular organelles lacking direct membrane continuity with the cell surface. An identical result was obtained for 8-cell and blastocyst stages.

Three types of organelle are found localized in the cytoplasm surrounding endosome clusters; their occurrence varies according to developmental stage. In oocytes and to a lesser extent at later stages, these comprise spherical multilayered membraneous whorls (0·2–0·5 μm diameter; Fig. 3A) which may also contain internalized vesicles (Fig. 3A; inset) suggesting that they are derived from endosomes undergoing senescence. In 2-cell and later staged embryos, endosome clusters commonly colocalize (without direct association) with closely packed granules (0·2–0·4 μm diameter) containing a homogeneous material and characterized by their densely stained apposed membranes ('jigsaw' granules of Calarco & Brown (1969); Fig. 2C). The granules appear to derive from cisternae of smooth endoplasmic reticulum during the 2-cell stage (Fig. 3B) and are ultimately autolysed at the morula stage during the formation of secondary lysosomes (see below). Endosome clusters in 4-cell embryos are occasionally associated with electron-dense 'degradative vacuoles'; these structures are more common in postcompaction stages (Figs 4B arrows, 5B,G) and appear to derive from endosomes.

All three procedures used for the cytochemical detection of acid hydrolases (acid phosphatase, pH 4·0, 5·2; aryl sulphatase, pH 4·0, 5·5; trimetaphosphatase, pH 3·9) gave negative results for these developmental stages despite a consistent positive localization for each technique in control mouse liver.

Fig. 2. Morphology and characteristics of endosomes. (A) Cluster of endocytotic vesicles within the cortical cytoplasm of a 2-cell embryo. Endosomes consist of a spherical or flattened vacuolar compartment (*v*) surrounded by smaller tubular or vesicular structures (*TVS*). Bar = 0·25 μm. (B) Endosome cluster from 2-cell embryo in which the vacuolar compartment (*v*) contains internalized vesicles (arrows). Bar = 0·23 μm. (C) Endosome closely associated with cytoplasmic 'jigsaw' granules (*g*) and showing membrane continuity (arrow) between vacuole (*v*) and *TVS* compartments. Bar = 0·25 μm. (D) Endosome with a deep invagination of the vacuole membrane (arrowheads) indicative of internalized vesicle (*ve*) formation. Bar = 0·25 μm. (E) Endosome characterized by an electron-dense 'mat' (arrow) associated with one region of the vacuole which is devoid of TVS elements. Bar = 0·25 μm. (F) Unstained section of the apposed region between blastomeres of a 2-cell embryo fixed in the presence of ruthenium red to label the cell membrane (arrows). Endosomes (*e*) are unstained by this process and therefore represent true intracellular organelles separate from the cell surface. Bar = 0·25 μm.

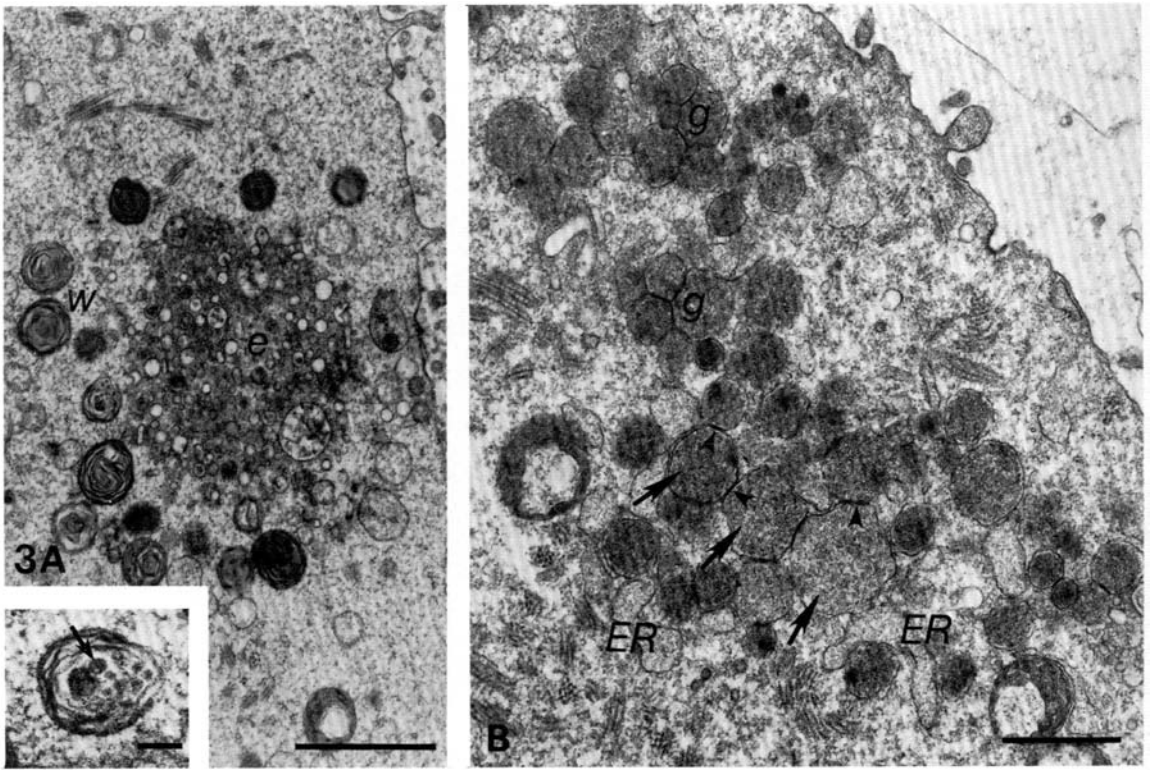

Fig. 3. (A) Endosome cluster (*e*) within an unfertilized oocyte; the complex is surrounded by a number of membraneous whorls (*w*), one of which is shown at higher magnification (inset) to contain internalized vesicles (arrow). Bar = 1 μm; inset = 0·1 μm. (B) Cortical region of cytoplasm from an early 2-cell embryo showing stages in the apparent formation of 'jigsaw' granules (*g*) from cisternae of smooth endoplasmic reticulum (*ER*). The granules derive from portions of the ER which exhibit a more rounded appearance and a progressive increase in electron density of their contents (arrows); in addition, apposed membranes show the characteristic high density staining (arrowheads) typical of mature granules. Bar = 0·5 μm.

8-cell stage

Endosome distribution

Throughout the 8-cell stage, the morphology of endosome clusters and their association with other organelles is similar to that of earlier stages; endosome distribution, however, alters at compaction. In early 8-cell embryos (2 h

Fig. 4. Endosome distribution during the 8-cell stage. (A) Region of an early 8-cell embryo (2 h post formation) showing endosome clusters (*e*) distributed predominantly in the cortical cytoplasm but with a small proportion occurring in the perinuclear area (arrow). Bar = 5 μm. (B) Blastomere from 1 h compacted 8-cell embryo with a polarized distribution of endosomes (*e*) in the apical cytoplasm beneath the microvillous pole (*mv*); arrows indicate occasional electron-dense degradative vacuoles. Bar = 5 μm.

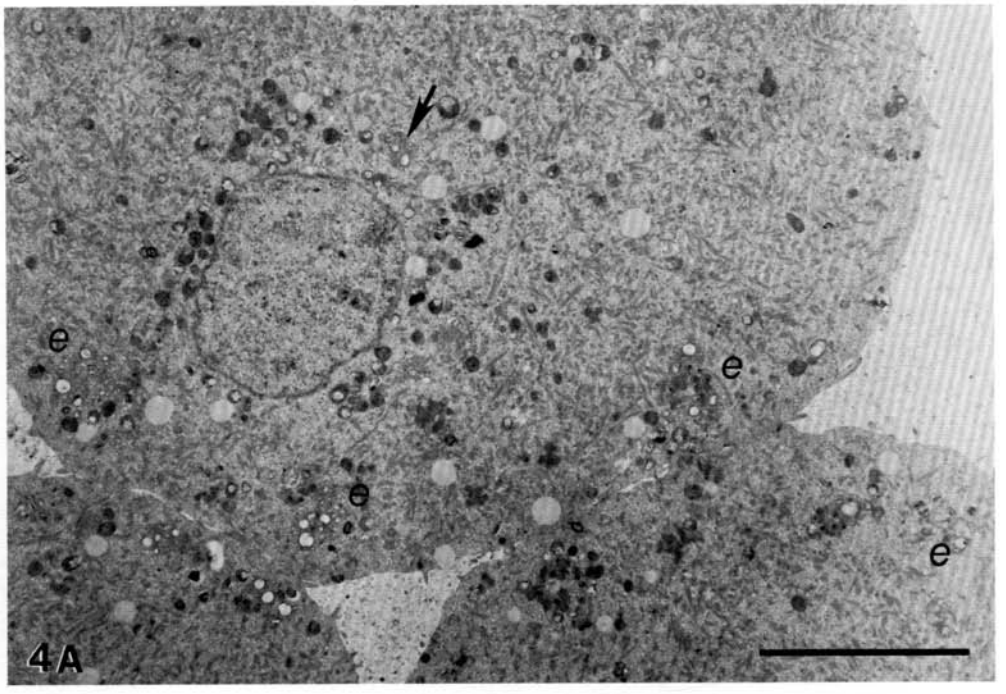
e
e
e
e
4A

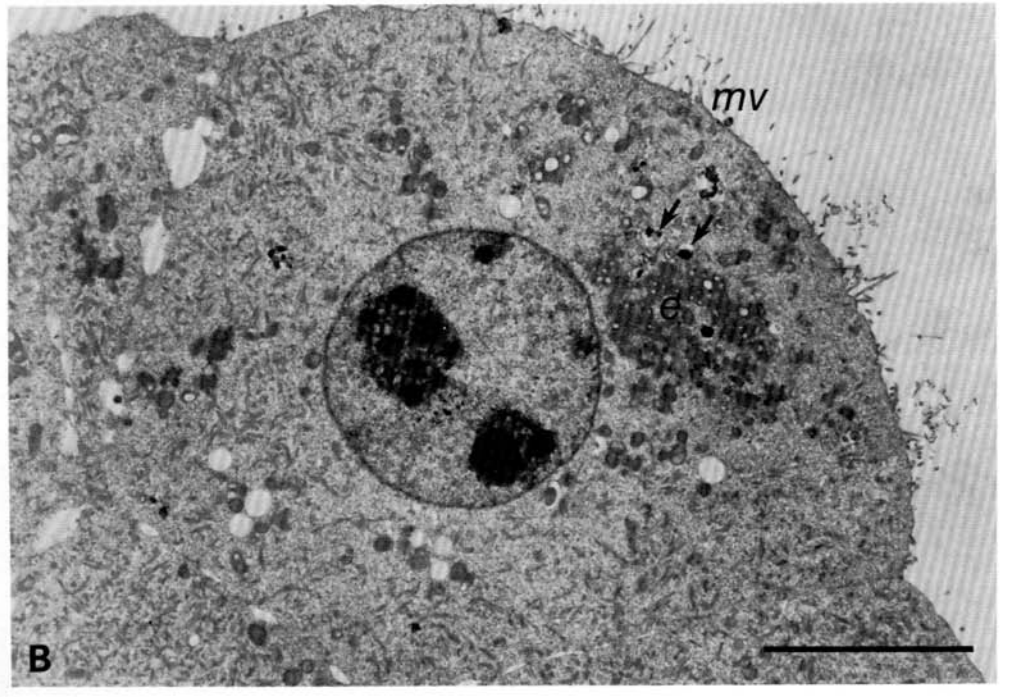
mv
e
B

postformation), endosomes are localized in two regions of the cell; (a) in the cortical cytoplasm and (b) in the perinuclear zone (Fig. 4A). Endosome counts made on electron micrographs of 48 blastomeres from intact 2 h 8-cell embryos have shown that approximately 80 % are cortical. The number of endosomes per unit area of apical and basal cytoplasm was likewise determined by analysing electron micrographs (Table 1). No significant difference in endosome localization was found between these two cytoplasmic zones, thus their distribution, as in earlier staged embryos, can be described as apolar.

In 1 h postcompaction 8-cell embryos, the distribution of endosomes is usually altered from the pattern described above. Endosomes, along with occasional degradative vacuoles and 'jigsaw' granules, tend to localize, but not exclusively, in a polar cluster in the apical cytoplasm above the nucleus and below the microvillous pole (Fig. 4B), thus correlating with the distribution pattern of HRP-labelled endocytotic organelles described for these cells by Reeve (1981*a*). The extent of endosome polarity in compacted 8-cell embryos is variable when whole cells/embryos are scored for its presence or absence at the light microscope level and has been evaluated at 55 % of embryos examined (Reeve, 1981*a*). In order to quantify the difference in the relative concentration of endosomes between apical and basal regions of the cell, an analysis of endosome number per unit area of cytoplasm was carried out on blastomeres from intact 1 h compacted embryos, comparable with that performed on early 8-cell embryos. The results (Table 1) show that endosome frequency in the apical cytoplasm is approximately twice that in the basal cytoplasm ($P < 0{\cdot}001$). Since there was no significant difference in endosome frequency for the whole cell between early and compacted 8-cell stages (Table 1), the process of polarization is likely to result from cytoplasmic relocation rather than by preferential assembly of endosomes in the apical region of the cell.

Table 1. *Mean endosome number/100 μm² cytoplasm* ± S.E. *derived from electron micrograph analysis of blastomeres from intact early 8-cell embryos (2 h post-formation), 1 h compacted 8-cell embryos and 9 h compacted 16-cell embryos (outside cells)*

Embryo stage	Whole cell (n)		Apical (A) cytoplasm		Basal (B) cytoplasm	Ratio A:B
early 8-cell	7·32 ± 0·60 (38)	NS	7·38 ± 0·73	−NS−	7·41 ± 0·76	0·996:1
compacted 8-cell	8·16 ± 0·51 (35)	*	10·72 ± 0·69	−**−	5·41 ± 0·62	1·982:1
outside 16-cell	12·10 ± 1·18 (37)		16·47 ± 2·23	−**−	7·51 ± 1·23	2·193:1

NS = not significant
* = $P < 0{\cdot}01$
** = $P < 0{\cdot}001$

Recent data on the role of the cytoskeleton in organizing endosome polarity (Fleming, Cannon & Pickering, 1985) support this view.

Processing pathway

The endocytotic processing pathway at the 8-cell stage was investigated by HRP labelling. Initially, intact 3 h 8-cell embryos were incubated in HRP-containing medium for a prolonged period (5 h) during which time they compacted, in order to label *all* components of the pathway. Before fixation, embryos was washed several times in M2+BSA to remove exogenous tracer (HRP is a 'content' marker and when unconjugated will not bind to membrane) so that all positive sites could reasonably be interpreted as intracellular. By this treatment, HRP was not found within the subzonal space nor between compacted cell membranes thus confirming the adequacy of the washing procedures. HRP was localized primarily in the endosome clusters (Fig. 5A) but was also found (a) within pinocytotic vesicles (PVs; 70 nm diameter) mainly distributed in the cortical cytoplasm close to the cell membrane but also occurring elsewhere, especially in the vicinity of endosome clusters (Fig. 5A), and (b) within degradative vacuoles when present, usually associated with endosome aggregates (Fig. 5B). At higher magnification, HRP within endosomes was restricted to the vacuolar compartment where it coated the inner surface of the membrane and surrounded internalized vesicles, but was not normally found within elements of the tubular and vesicular structures (Fig. 5C, TVS). Comparable labelling patterns have been obtained with anionic ferritin (data not shown).

The time course of the processing pathway was investigated in early (2 h postformation) and late (1 h postcompaction) 8-cell embryos incubated in HRP for periods varying between 1–40 min. After 1 min incubation, endosomes were unlabelled but infrequent positive pinocytotic vesicles were detected beneath the cell membrane. By 5 min incubation, positive PVs were found both in the vicinity of the membrane and deeper within the cytoplasm close to or fusing with endosomes (Fig. 5D,E), of which a small number within each cluster was labelled. The proportion of endosomes labelled following HRP incubations for 5, 10 and 20 min was compared between early and compacted 8-cell embryos by analysis of electron micrographs (Table 2). For both stages, the proportion of HRP-positive endosomes increased significantly with time, with approximately 70–75 % containing HRP by 20 min incubation. However there was no significant difference between early and compacted embryos, nor between endosomes localized in the apical *versus* the basal cytoplasm, for either stage. Degradative vacuoles remained unlabelled following incubations for up to 20 min, but a number contained HRP by 30–40 min incubation.

The nature of the processing pathway linking endosomes with degradative vacuoles is obscure since, in contrast to the labelling of endosomes by pinocytotic vesicles described above, HRP-containing vesicles (endosome or cell membrane derived) were not observed to fuse with degradative vacuoles. However, amongst

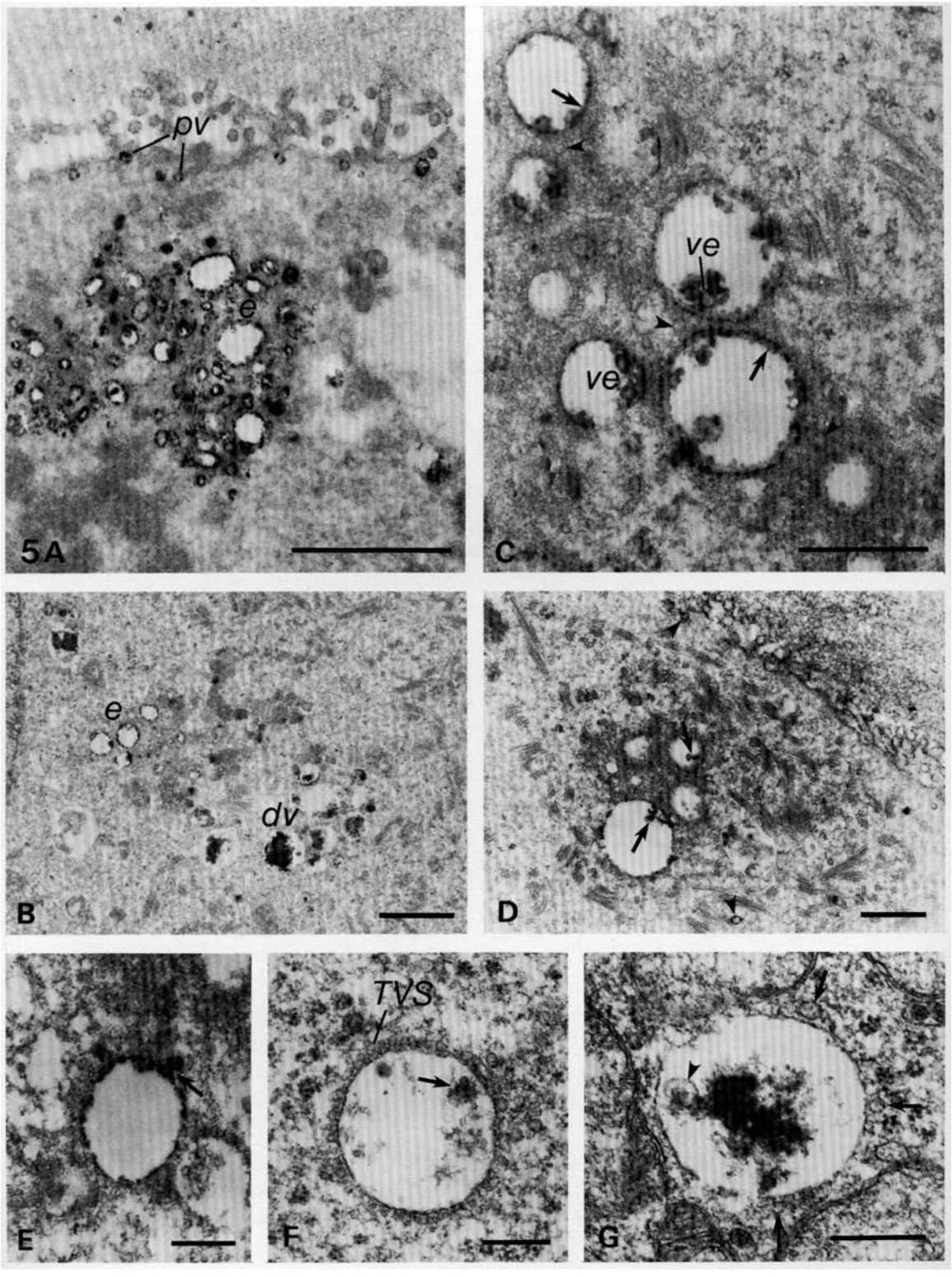
pv
e
5A
ve
ve
C
e
dv
B
D
TVS
E
F
G

the population of endosomes found either within the apical pole or localized elsewhere, a number was observed with an intermediate morphology showing (a) an increase in size, (b) an accumulation of electron-dense material and (c) a reduction or loss of tubular and vesicular structures (Fig. 5F,G,). Thus, it is likely that degradative vacuoles acquire tracer by a process of endosome transformation.

All techniques used for the localization of lysosomal hydrolases gave negative results in both early and compacted 8-cell blastomeres (Fig. 9D).

The endocytotic processing pathway at earlier stages (oocyte to 4-cell stage) was found not to differ from that described above.

Timing of endosome polarization

The time at which endosome polarization occurs during the fourth cell cycle was investigated in natural 2/8 couplets cultured from division of 1/4 blastomeres over the period 0–8 h and observed at hourly intervals. In order to correlate this event with surface polarization of microvilli, cells were both preincubated in HRP to label the endosome compartment and stained subsequently by indirect immunofluorescence to label the cell surface; results are shown in Table 3.

The majority of cells aged up to 5 h postdivision were found to be apolar for both HRP localization and surface staining (Table 3; column 3; Fig. 6A). However, an increasing number of cells show apical polarization of endosomes from 4 h postdivision (column 7) whereas a comparable rise in the incidence of surface polarization is not evident until 6 h postdivision (column 8). During this period (4–6 h) there is a sizeable population of cells (approximately 25 %) which are only polarized for endosome localization (column 4; Fig. 6B). Following culture for 7–8 h, the incidence of surface polarity exceeds that of endosome polarity (compare columns 7 and 8) and a subpopulation of cells showing only surface polarity is now evident (column 5; Fig. 6D). In the major cell

Fig. 5. (A–E) Unstained sections of 8-cell embryos incubated in HRP. (A) Region of the apical cytoplasm of compacted embryo incubated in HRP for 5 h prior to washing and fixation. The tracer is found within clusters of endosomes (*e*) and pinocytotic vesicles (*pv*) localized close to the apical membrane and amongst the endosome vacuoles. Bar = 1 μm. (B) Detail of cytoplasm from compacted embryo treated in a similar manner to (A) above. In addition to endosomes (*e*), HRP is also localized within degradative vacuoles (*dv*). Bar = 1 μm. (C) Detail of compacted 8-cell cytoplasm similar to (A) and (B) above showing HRP lining the inner surface of the endosome vacuole (arrows) and surrounding internalized vesicles (*ve*); elements of the TVS (arrowheads) are not labelled. Bar = 0·5 μm. (D) Cytoplasmic region of compacted embryo incubated in HRP for 5 min before fixation. The tracer is already present inside two of the four endosomes shown (arrows) and within pinocytotic vesicles (arrowheads) adjacent to the cell surface or deeper within the cytoplasm close to the endosome cluster. Bar = 0·5 μm. (E) HRP-labelled endosome from compacted 8-cell embryo incubated in tracer for 5 min; arrow denotes fusion between a pinocytotic vesicle and the endosome vacuole. Bar = 0·25 μm. (F),(G) Proposed stages in the transformation of endosomes into degradative vacuoles. (F) Endosome surrounded by a distinct TVS compartment but containing electron-dense material within the vacuole lumen (arrows). Bar = 0·25 μm. (G) Degradative vacuole stage with remnant of TVS system (arrows) and additional dense material, including an internalized vesicle (arrowhead) within the lumen. Bar = 0·5 μm.

Table 2. *The percentage of endosomes labelled by HRP incubations within apical, basal and total cytoplasm of blastomeres from early 8-cell embryos (2 h postformation), 1 h compacted 8-cell embryos and 9 h compacted 16-cell embryos (outside blastomeres). Analyses conducted on electron micrographs*

Embryo stage	HRP incubation time (min)	% HRP labelled endosomes: whole cell (n)		apical cytoplasm		basal cytoplasm
early 8-cell	5	31·6(14)	**	34·5	–NS–	16·9
	10	59·7(16)	*	62·9	–NS–	55·7
	20	75·0(22)		80·0	–NS–	76·0
compacted 8-cell	5	22·9(17)	**	22·1	–NS–	20·7
	10	54·8(18)	**	53·5	–NS–	63·5
	20	70·5(17)		76·4	–NS–	65·6
outside 16-cell	10	61·2(19)	*	64·1	–NS–	56·6
	20	77·0(18)		80·8	–NS–	80·8

NS = not significant
* = $P < 0{\cdot}01$
** = $P > 0{\cdot}001$
Statistical comparisons were made using Student's t test on means and S.D.s of arcsin transformed individual values.

subpopulation, however, both types of polarization are evident (column 6; Fig. 6C). Where both features of polarity are present they colocalize and are almost always opposite to the point of intercellular contact, confirming the observation of Reeve (1981*a*).

From these results we conclude that endosome polarization usually *precedes* surface polarization by 1–2 h but that the period over which the former event occurs for a population of cells may be longer than that required for the establishment of surface polarization.

Polarity of endocytotic pathway

The preferential localization of endosomes within the apical cytoplasm and below the microvillous pole in compacted 8-cell blastomeres is suggestive of a polarization of the endocytotic pathway to this region of the cell. To determine whether pinocytotic activity occurs preferentially at the apical membrane compared to the basolateral cell surface, the number of pinocytotic vesicles (PVs) (labelled by HRP incubation) localized within 0·5 μm of either of these two domains was ascertained and standardized to a unit length of cell membrane (= index of pinocytosis, IP; see Materials & Methods). The data for early, compacted and decompacted 8-cell embryos are given in Table 4.

Although in compacted embryos the index of pinocytosis for apical membrane is greater than that for basolateral membrane following HRP labelling for 5 or 10 min, the difference is not significant. However, when embryos are incubated in

HRP for 20 min, by which time the number of membrane-associated PVs has increased, this difference is significant ($P < 0{\cdot}01$) and represents a 50 % increase in pinocytotic activity at the apical surface over that at the basolateral surface. Comparative data for early 8-cell embryos following 5, 10 or 20 min incubations show no significant difference in pinocytotic activity between apical and basolateral membranes. Since the data for the whole cell do not differ between early and compacted embryos (for all incubation periods), the elevated level of apical pinocytosis in compacted cells detectable after 20 min incubation is more likely to represent a *clustering* of membrane regions involved in endocytosis to the apical membrane rather than an increase *per se* in the number of such sites at the cell apex. The difference in pinocytotic activity between apical and basolateral membranes at compaction is not a reflection of limited accessibility of tracer since

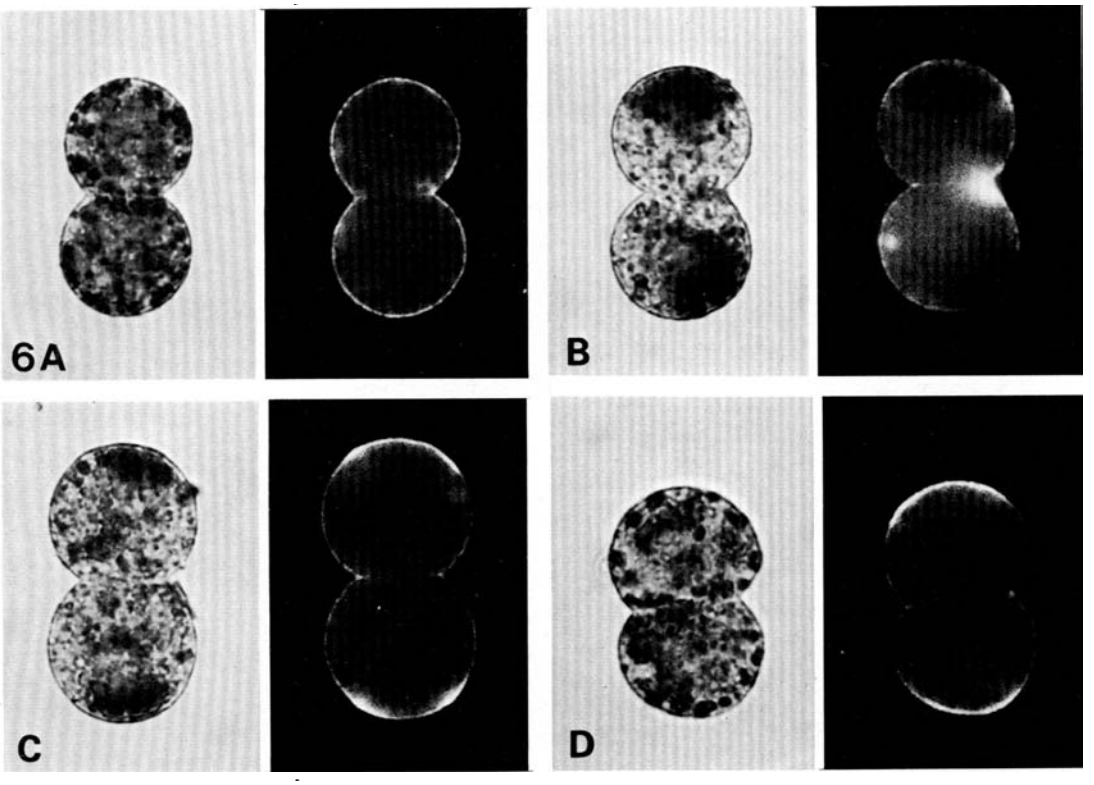

Fig. 6. Light micrographs of prelabelled 2/8 couplets derived from *in vitro* division of 1/4 cells and cultured for varying periods to determine the relative times of endosome and surface polarization. Bright-field image demonstrates HRP sites corresponding to endosome clusters; fluorescent image denotes surface microvillous labelling following RAMS-FITC GAR staining. For quantification of data, see Table 3. (A) 2/8 couplet cultured for 2 h from division showing an apolar distribution of both HRP sites and surface label. (B) 6 h cultured couplet showing apical polarization of HRP sites and an apolar distribution of surface label. (C) 6 h cultured couplet in which both HRP and surface label are polarized apically. (D) 7 h cultured couplet showing polarized surface labelling but an apolar distribution of HRP. (Mag. ×380).

a comparable ratio (1·59:1, apical:basolateral IP, 20 min incubation) is obtained when decompacted embryos are analysed. Both apical and basolateral pinocytotic indices are, however, equally reduced in decompacted embryos compared with compacted stages and this reduction is likely to result from the inhibitory effects of low Ca^{2+} medium on endocytosis (Duncan & Lloyd, 1978).

16-cell morulae and later stages.

Endosome distribution

Outside blastomeres from relatively early 16-cell embryos (9 h postcompaction) usually exhibit a polar distribution of endosomes in the apical cytoplasm in a manner comparable with compacted 8-cell stages (Fig. 7). Cells that appear inside possess apolar endosome clusters reminiscent of the condition in early 8-cell embryos (Fig. 7). Analysis of endosome number per unit area of cytoplasm in outside cells (Table 1) demonstrates a significant difference ($P < 0{\cdot}001$) in the relative concentration of these organelles between apical and basal zones of the cell with a ratio (2·2:1) which exceeds that obtained for the compacted 8-cell stage. Furthermore, the concentration of endosomes in the total cytoplasm is higher ($P < 0{\cdot}01$) than in 8-cell stages, indicating either an increase in endosome formation or their differential segregation to outer polar cells at division.

Processing pathway

The characteristics of endosome labelling following HRP incubation in outside 16-cell blastomeres did not show differences from the 8-cell stage (Table 2). The proportion of endosomes labelled after 10 and 20 min incubations (61 % and 77 %

Table 3. *Incidence of polarized HRP localization (endosome polarity) and FITC labelling (surface polarity) in natural 2/8 couplets cultured for varying times from division* in vitro *of 1/4 cells*

		Incidence of endosome and surface polarity (%)					
Time post division (h)	Cell number	endosomes and surface *apolar*	endosomes *polar* surface *apolar*	endosomes *apolar* surface *polar*	endosomes and surface *polar*	total endosome polarity	total surface polarity
0	47	95·7	2·1	0	2·1	4·2	2·1
1	60	91·7	1·7	0	6·7	8·3	6·7
2	77	79·2	13·0	3·9	3·9	16·9	7·8
3	116	87·1	7·7	0·9	4·3	12·1	5·2
4	72	72·2	25·0	0	2·8	27·8	2·8
5	126	61·1	23·8	0	15·1	38·9	15·1
6	50	34·0	24·0	12·0	30·0	54·0	42·0
7	61	13·1	14·7	22·9	49·2	63·9	72·1
8	53	13·2	11·3	34·0	41·5	52·8	75·5
column no.							
1	2	3	4	5	6	7	8

respectively) was higher, but not significantly so, than the comparable data obtained for the compacted 8-cell stage. Similarly, there was no significant difference between apical and basal populations of endosomes with respect to the percentage labelled for either incubation time.

Polarity of endocytotic pathway

The relative pinocytotic activity (IP) of apical and basolateral faces of outside 16-cell blastomeres was assessed following HRP labelling for 10 or 20 min using the same procedure employed at the 8-cell stage (Table 5). The IP of apical membrane was significantly higher ($P < 0{\cdot}001$) than that of basolateral membrane at both incubation times, with a ratio approximating 2:1. Thus a sharper distinction is evident in endocytotic activity between apical and basolateral surfaces in polar 16-cells than in polar 8-cells, yet the total cell activity for both stages is not significantly different, suggesting that the polarization of the endocytotic pathway is accomplished by a continuous clustering of pre-existing membrane sites involved in endocytosis to the apical surface. In control (decompacted) 16-cell embryos, apical and basolateral IPs are significantly different ($P < 0{\cdot}001$) with ratios comparable with those obtained for experimental embryos; thus preferential apical endocytosis is not attributable to limited accessibility of HRP to basolateral

Table 4. *Mean indices of pinocytosis (IP)* ± S.E. *at apical and basolateral membrane domains of blastomeres from intact early 8-cell embryos (2 h postformation), 1 h compacted embryos and 1 h decompacted embryos. IP = pinocytotic vesicle number/10 μm membrane following HRP labelling for a standardized time*

HRP incubation time		early 8-cell (n)		compacted 8-cell (n)		decompacted 8-cell (n)	
5 min	A	0·541 ± 0·077	NS	0·605 ± 0·105	NS	0·504 ± 0·118	NS
	B	0·543 ± 0·052		0·419 ± 0·063		0·390 ± 0·078	
	A+B	0·536 ± 0·058	−NS−	0·504 ± 0·075	−NS−	0·435 ± 0·085	
	R	0·995:1		1·444:1		1·293:1	
		(16)		(17)		(14)	
10 min	A	1·501 ± 0·143	NS	1·626 ± 0·237	NS	1·120 ± 0·260	NS
	B	1·570 ± 0·159		1·553 ± 0·175		0·831 ± 0·172	
	A+B	1·541 ± 0·117	−NS−	1·590 ± 0·190	−**−	0·937 ± 0·205	
	R	0·956:1		1·047:1		1·347:1	
		(16)		(18)		(14)	
20 min	A	2·246 ± 0·186	NS	3·119 ± 0·334	*	1·764 ± 0·189	*
	B	2·278 ± 0·214		2·073 ± 0·151		1·108 ± 0·101	
	A+B	2·259 ± 0·175	−NS−	2·544 ± 0·183	−***−	1·381 ± 0·088	
	R	0·986:1		1·504:1		1·592:1	
		(22)		(17)		(18)	

A IP of apical membrane
B IP of basolateral membrane
A+B IP of whole membrane
R ratio of A:B

NS = not significant
* = $P < 0{\cdot}01$
** = $P < 0{\cdot}005$
*** = $P < 0{\cdot}001$

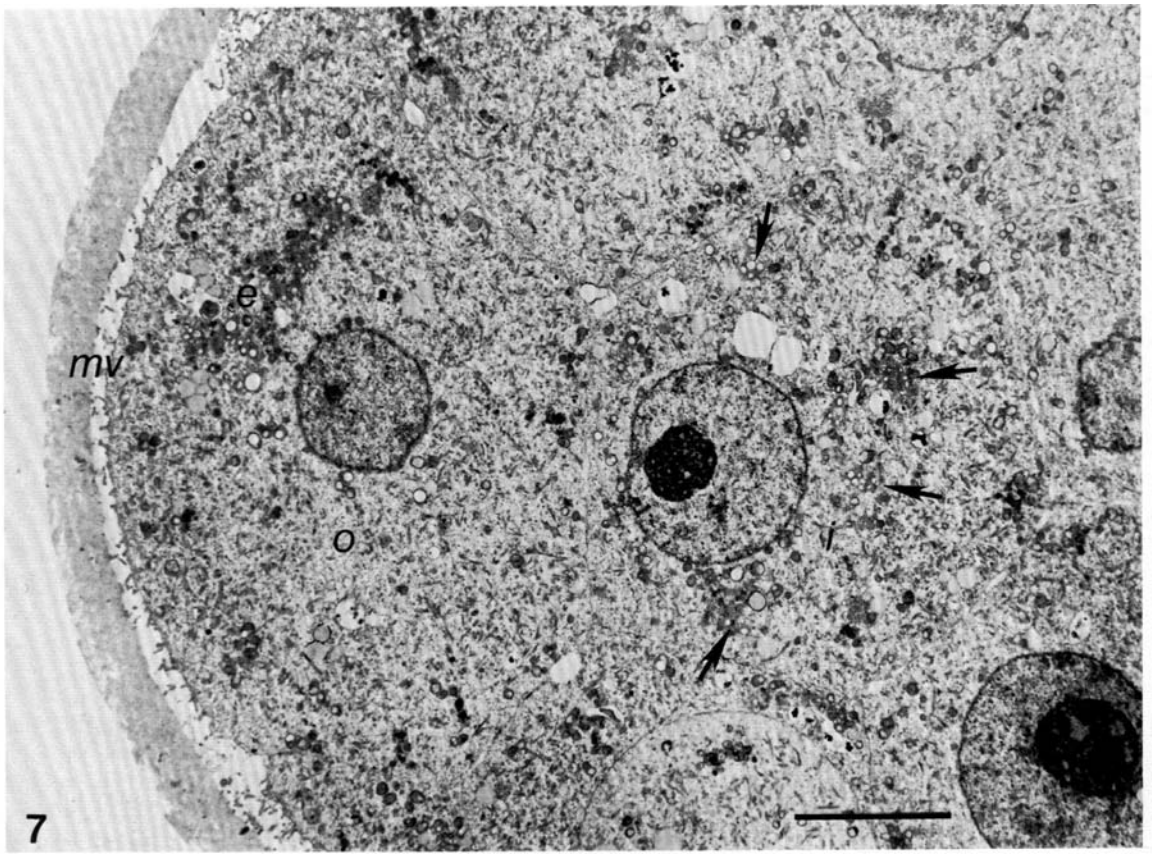

Fig. 7. Region of 16-cell embryo fixed at 9 h postcompaction. The outside cell (*o*) shows a polar distribution of endosomes (*e*) beneath the apical microvillous surface (*mv*), whereas the enclosed cell (*i*) contains small, apolar endosome aggregates (arrows). Bar = 5 μm.

surfaces. Interestingly, the inhibitory effect of external calcium deficiency on endocytosis noted in decompacted 8-cell embryos was not apparent at the 16-cell stage. The IP data for trophectoderm cells within mid-expanded blastocysts (Table 5) demonstrate a further increase in the polarization of the endocytotic pathway with the number of profiles of pinocytotic vesicles at the apical membrane exceeding those at the basolateral surface by a ratio greater than 3:1 for both incubation times.

Secondary lysosome formation and polarization

During the later period of the 16-cell stage, and continuing into the 32-cell stage, a further maturation of the endocytotic apparatus is evident in both outside and enclosed cells. These events culminate in the formation of a pool of secondary lysosomes which, in outside blastomeres, are polarized in the basal region of the

cell. A description of these changes will precede the data quantifying their time of occurrence.

Outside blastomeres from embryos aged 9–25 h postcompaction (early/mid 16-cell to mid 32-cell stages) display a reorganization in the distribution of several cytoplasmic organelles which become localized in the basal cytoplasm (Fig. 8A). These structures may include mitochondria, endosome clusters, cytoplasmic ('jigsaw') granules, crystalline arrays, lipid droplets, Golgi bodies and degradative vacuoles (Fig. 8B). The basal aggregates of cytoplasmic granules (which in early cleavage stages colocalize with endosome clusters and are characterized by electron-dense membranes, see Fig. 2C) undergo a process of autolysis which involves (a) their isolation from surrounding cytoplasm resulting in the formation of artifactual lucent spaces and (b) the breakdown of their limiting membranes and the progressive increase in electron density of their contents (Fig. 8B). The end product of granule autolysis is a heterogeneous, electron-dense structure (secondary lysosome, see below) of comparable morphology to the degradative vacuoles already described. During the 16- to 32-cell stage these accumulate progressively in the basal cytoplasm of outside cells (Fig. 9A), but occur in a more random distribution within enclosed cells. An apical pole of endosomes is however retained in outside blastomeres (Fig. 9A), although it is normally of smaller size compared with the early 16-cell condition. In cavitated embryos, the apicobasal disposition of endocytotic organelles in outside (trophectoderm) cells is

Table 5. *Mean indices of pinocytosis (IP) ± S.E. at apical and basolateral membrane domains of outside blastomeres from intact compacted and decompacted 16-cell embryos (9 h postcompaction) and 6 h postcavitation blastocysts. IP = pinocytotic vesicle number/10 μm membrane following HRP labelling for a standardized time. Blastocysts were collapsed with a microinjection electrode 45 min prior to incubation in order to equalize HRP accessibility to both membrane faces*

HRP incubation time	compacted 16-cell (n)		decompacted 16-cell (n)		blastocyst (n)	
10 min	A 2·158 ± 0·244	***	A 2·562 ± 0·179	***	A 4·335 ± 0·466	***
	B 1·102 ± 0·138		B 1·069 ± 0·117		B 1·374 ± 0·183	
	A+B 1·495 ± 0·140	−NS−	A+B 1·662 ± 0·097		A+B 2·479 ± 0·290	
	R 1·958:1		R 2·395:1		R 3·153:1	
	(19)		(19)		(21)	
20 min	A 4·051 ± 0·369	***	A 4·351 ± 0·377	***	A 5·663 ± 0·505	***
	B 2·038 ± 0·249		B 2·213 ± 0·281		B 1·744 ± 0·150	
	A+B 2·885 ± 0·184	−NS−	A+B 3·192 ± 0·268		A+B 3·193 ± 0·220	
	R 1·988:1		R 1·966:1		R 3·247:1	
	(18)		(20)		(22)	

A IP of apical membrane
B IP of basolateral membrane
A+B IP of whole membrane
R ratio of A:B

NS = not significant
*** = $P < 0{\cdot}001$

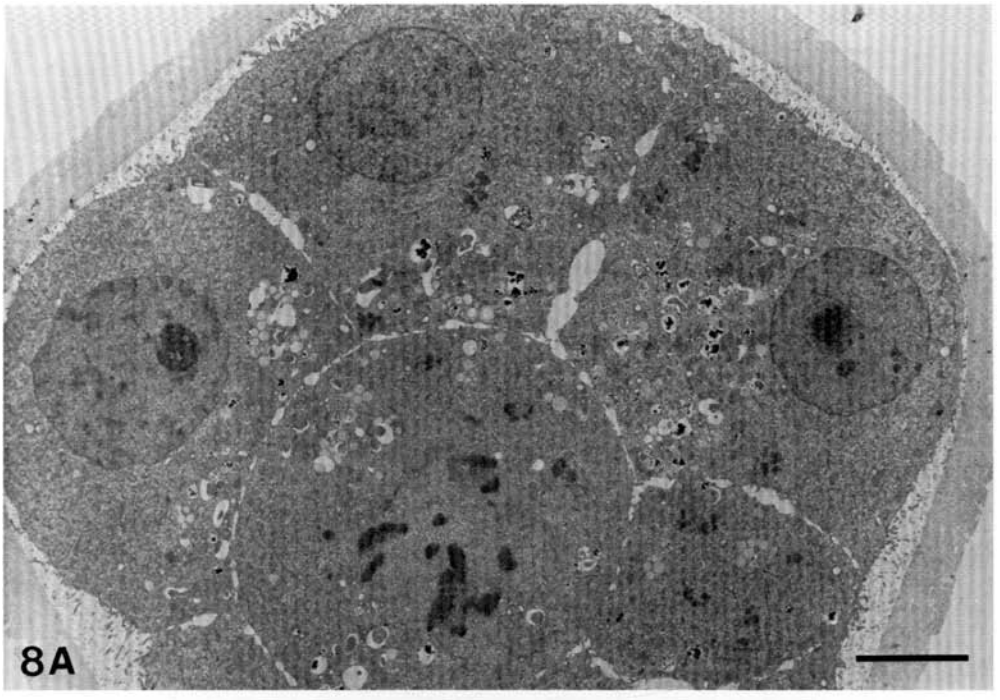
8A

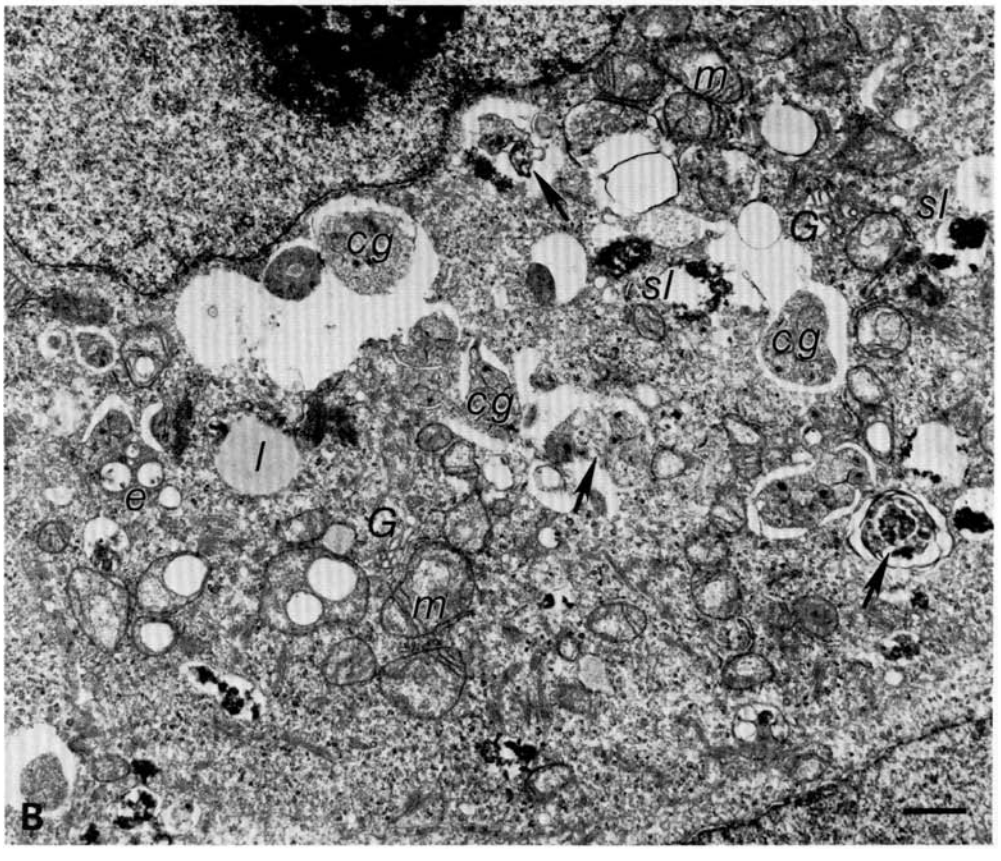
m
G
sl
cg
sl
cg
cg
l
e
G
m
B

unchanged; electron-dense secondary lysosomes are evident particularly within basal TE processes which cover the juxtacoelic face of the ICM (Fleming *et al.* 1984).

Cytochemical examination of 16-cell morulae (12 h postcompaction) and midexpanded blastocysts for lysosomes failed to detect unambiguous acid phosphatase or aryl sulphatase activity but a positive trimetaphosphatase reaction (negative in controls) was obtained consistently in the growing population of basal electron-dense vacuoles, (Fig. 9B), including those located within juxtacoelic processes (Fig. 9C), thus demonstrating their secondary lysosome status. Endosomes and intact aggregates of cytoplasmic granules were non-reactive for trimetaphosphatase.

When late 16-cell morulae are incubated in HRP, the tracer becomes localized within the forming population of basal secondary lysosomes after 30–40 min (Fig. 9E). (See Fleming *et al.* (1984) for evidence of HRP localization within the more substantial pole of basal lysosomes in early blastocysts.) For those embryos fixed directly from the incubation medium, HRP is retained in regions of cell contact (Fig. 9E) thus demonstrating the paracellular movement of the tracer and confirming that lysosome polarization precedes zonular tight junction formation.

Timing of secondary lysosome polarization

The timing of the events leading to the formation and basal polarization of secondary lysosomes within outside blastomeres was examined in ultrasections of intact 16- to 32-cell morulae timed from compaction (range 9–25 h) prior to fixation. Cells (sectioned through the nucleus) were scored for the presence or absence of a basal pole of (a) granules undergoing autolysis and (b) secondary lysosomes (Fig. 10). Basal localization of lysosomes was first detected in a minority of outside cells at 10 h postcompaction and reached a maximum of 75–80 % by 17 h postcompaction; the proportion of cells displaying granule degradation began to decline from 21 h postcompaction.

A more precise timing of basal localization of secondary lysosomes in relation to the fifth cell cycle was determined by experiments on *in vitro* cultured cell pairs. Blastomeres derived from compacted 8-cell embryos were cultured individually in the presence of HRP to label the endocytotic organelles and examined hourly for division to 2/16 couplets. These were cultured for varying periods (0–12 h) during the fifth cell cycle in Ca^{2+}-free medium to prevent intercellular flattening and envelopment (Ziomek & Johnson, 1981) and surface labelled for the detection of the microvillous pole prior to fixation, HRP development and examination. In

Fig. 8. (A) Low-power micrograph of mid-morula stage (15 h postcompaction); outside cells demonstrate the polarization of several organelles in the basal cytoplasm. Bar = 5 μm. (B) Basal cytoplasm of outside 16-cell blastomere (13 h postcompaction). Organelles polarizing in this region of the cell include mitochondria (*m*), lipid (*l*), Golgi bodies (*G*), endosomes (*e*) and aggregates of cytoplasmic 'jigsaw' granules (*cg*). The granules become isolated from the surrounding cytoplasm resulting in the formation of artifactual spaces; granule contents show evidence of degradation (arrows) leading to the formation of electron-dense secondary lysosomes (*sl*). Bar = 1 μm.

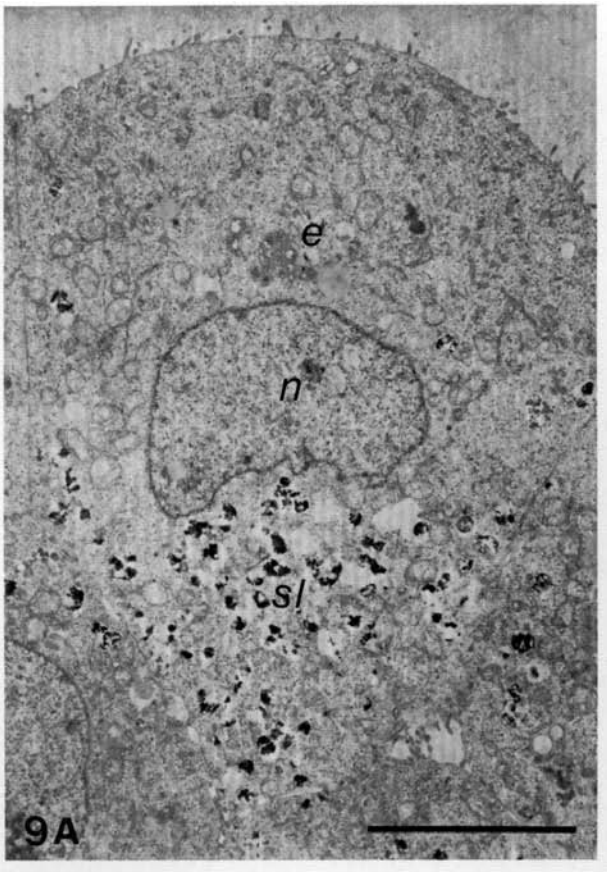
e
n
sl
9A

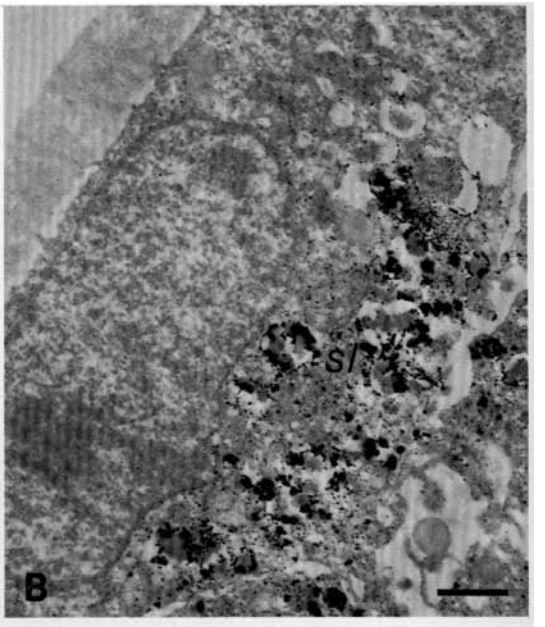
sl
B

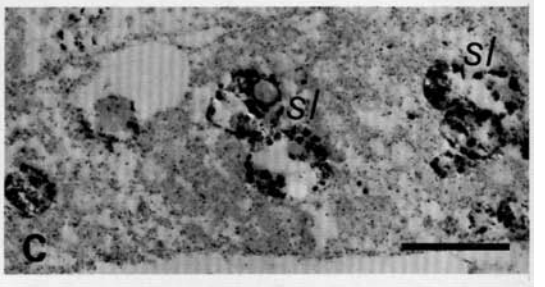
sl
sl
C

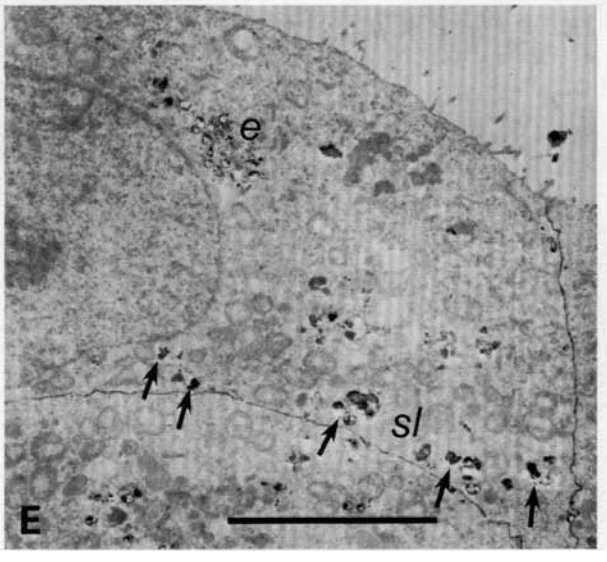
e
sl
E

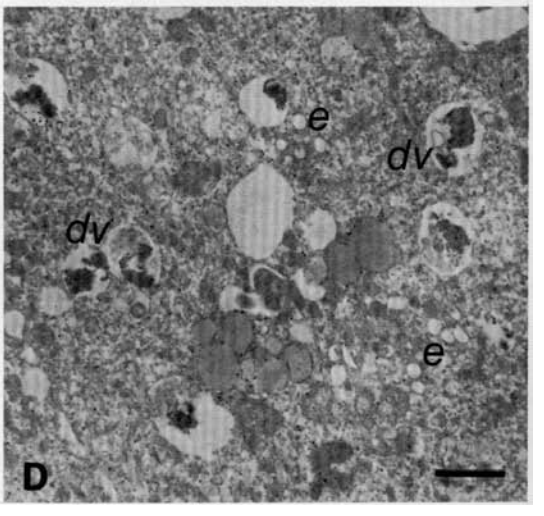
e
dv
dv
e
D

most (83 %) couplets, one cell was clearly larger than its companion. Since larger cells from natural 2/16 couplets have been shown to represent the *in vitro* equivalent of polar outside cells in 95 % of cases (Johnson & Ziomek, 1981), such cells with polar surface labelling were scored for the distribution of HRP within the cytoplasm (Table 6). However, the orientation of the division plane of 1/8 cells in culture is variable and may bisect the surface pole thereby generating two polar daughter cells (Fig. 11A). Thus the position of the inherited surface pole may bear little relation to the point of intercellular contact. HRP distribution in larger polar cells was therefore scored with the microvillous pole acting as a reference point for the apex of the cell.

In the majority of larger polar cells, HRP sites were preferentially localized within one region of the cytoplasm (focal, Table 6, columns 4–7). With few exceptions, such cells displayed HRP polarized either in the apical cytoplasm corresponding to the pole of endosomes (column 4, Fig. 11C) or in the basal cytoplasm corresponding to the pole of secondary lysosomes (column 5, Fig. 11D); only in a minority of cases were focal HRP sites distributed elsewhere (columns 6,7). In the 0 h culture group however, a substantial proportion (44 %) of larger cells with a polar surface phenotype displayed an apolar or ambiguous disposition of HRP (Fig. 11B) indicating that the spatial organization of the endocytotic system is not maintained continuously during cytokinesis but becomes re-established subsequently.

Comparison between columns 4 and 5 of Table 6 shows that during the 12 h culture period, there is a shift with time in the predominant form of HRP localization from the apical cytoplasm (endosomes) to the basal cytoplasm (secondary lysosomes), with the transition to the latter pattern occurring by 9 h postdivision. These results are therefore consistent with those obtained from sectioned material (Fig. 10) considering that division to the 16-cell stage is likely to occur from 2 to 4 h postcompaction.

Effect of exogenous protein concentrations on secondary lysosome polarization

Late 2-cell embryos (48 h post-hCG) were cultured up to the late 8-cell stage (1 h postcompaction; 70–72 h post-hCG), the early 16-cell stage (6 h

Fig. 9. (A) Outside cell from late morula (19 h postcompaction) showing a distinct pole of electron-dense secondary lysosomes (*sl*) in the basal cytoplasm. An apical cluster of endosomes (*e*) is located above the nucleus (*n*). Bar = 5 μm. (B–D) Unstained sections of embryonic stages following trimetaphosphatase cytochemistry. (B) Polar trophectoderm cell from early blastocyst in which the reaction product is localized in the basal cytoplasm associated with the secondary lysosome (*sl*) population. Bar = 1 μm. (C) Trophectodermal process showing trimetaphosphatase reactivity associated with secondary lysosomes (*sl*). Bar = 1 μm. (D) Region of compacted 8-cell cytoplasm; endosomes (*e*) and degradative vacuoles (*dv*) are non-reactive for trimetaphosphatase. Bar = 1 μm. (E) Outside cell from 16-cell embryo (15 h postcompaction) incubated in HRP for 40 min before immediate fixation. The tracer is localized within the apical pole of endosomes (*e*) and within basal secondary lysosomes (*sl*, arrows); it is also retained in intercellular spaces indicating that zonular tight junctions have not yet developed. Bar = 5 μm.

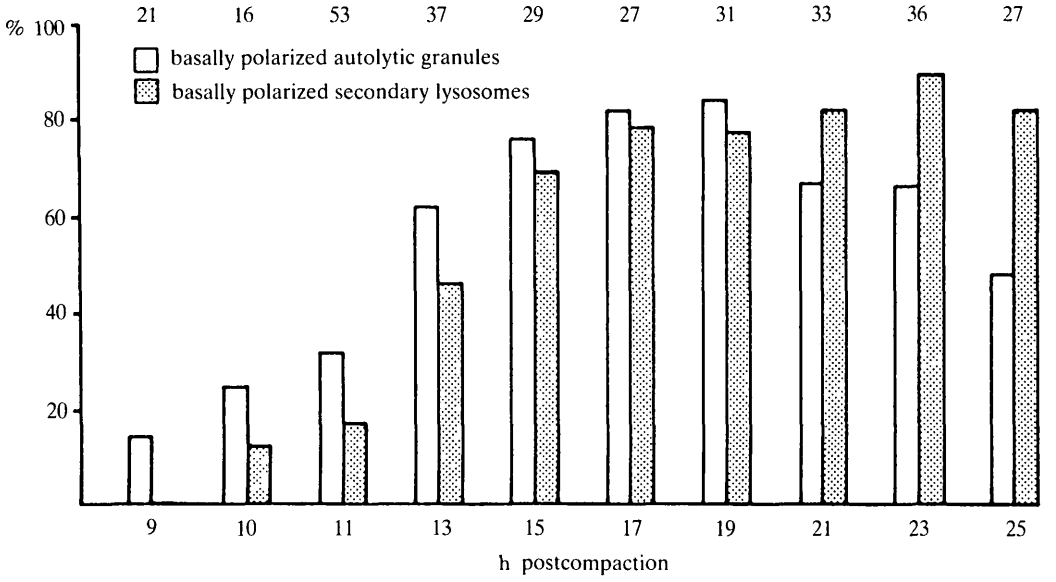

Fig. 10. Timing of secondary lysosome formation in outside cells of morulae aged 9–25 h postcompaction. Cells were scored in ultrasections of morulae for the presence or absence of basally polarized granule autolysis and electron dense secondary lysosomes. The numbers of cells examined are given above each time point.

postcompaction; 75–78 h post-hCG) or the late 16-/early 32-cell stage (15 h post-compaction; 84–88 h post-hCG) in M16 containing an elevated concentration of BSA (20 mg ml^{-1}) to examine whether the timing of basal polarization of secondary

Table 6. *Distribution patterns of HRP in larger, polar cells from prelabelled natural 2/16 couplets cultured for varying times from division* in vitro *of 1/8 cells*

Time post division (h)	Cell number	Incidence of HRP distribution patterns (%)				
			Focal*			
		Apolar	apical	basal	apical + basal	lateral
0	57	43·9	40·3	8·8	0	7·0
3	66	6·1	75·7	15·1	0	3·0
5	48	22·9	62·5	12·5	0	2·1
7	86	7·0	58·1	27·9	7·0	0
9	67	1·5	38·8	47·7	10·4	1·5
12	78	9·0	19·2	61·5	3·8	6·4
1	2	3	4	5	6	7 column

*Focal HRP distribution scored in relation to the position of the apical microvillous pole detected by indirect immunofluorescence.

lysosomes in outside cells, normally occurring during the late morula stage, could be influenced by the relative amount of exogeneous protein endocytosed during cleavage. At the two earlier stages, there was a marked increase in the number of electron-dense vacuoles found within the cytoplasm compared with control embryos cultured in M16+4 mg ml^{-1} BSA. However, these were consistently situated in the *apical* cytoplasm associated with the endosome poles (Fig. 12); only in the later staged embryos, including controls, were secondary lysosomes localized basally. Thus the timing of the maturation of the endocytotic pathway appears to be relatively independent of environmental factors and therefore is likely to represent an integral stage in the temporally regulated developmental programme leading to the formation of a polarized epithelium.

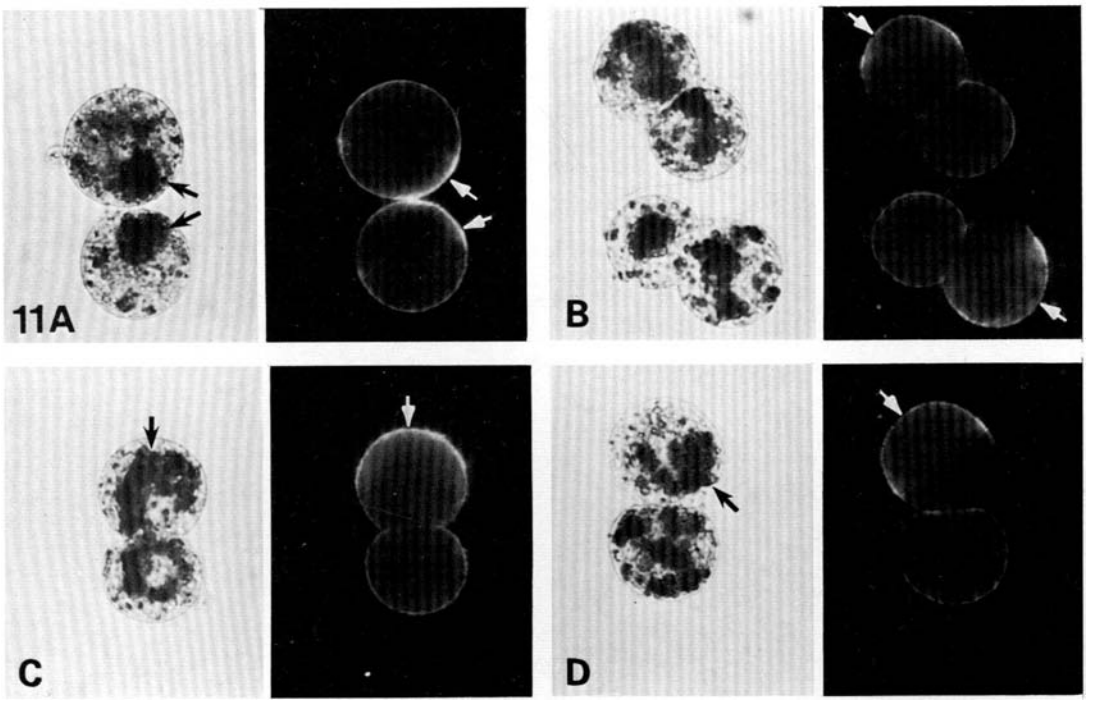

Fig. 11. Light micrographs of prelabelled 2/16 couplets derived from *in vitro* division of 1/8 cells and cultured for varying periods to determine the changing pattern of HRP localization during the cell cycle in larger surface polar cells visualized by indirect immunofluorescence. Black arrow = HRP pole, white arrow = surface pole. For quantification of data, see Table 6. (A) 3 h cultured 2/16 couplet in which the plane of division has bisected the surface pole thereby generating two polar daughter cells; in both cells, HRP is localized directly beneath the surface pole corresponding to the polar cluster of endosomes in the apical cytoplasm. (B) Two couplets immediately following division (0 h group) in which the larger cells showing polar surface labelling contain an ambiguous or apolar distribution of HRP. (C) 3 h cultured 2/16 couplet in which the larger surface polar cell contains apically polarized HRP sites which envelop the nucleus. (D) 9 h cultured 2/16 couplet in which the larger surface polar cell contains basally polarized HRP sites corresponding to the secondary lysosome pole. (Mag. ×380).

DISCUSSION

Our studies on the early developmental stages of the mouse embryo have shown that during cleavage the endocytotic system undergoes two accompanying cellular processes, namely (a) the maturation of the lysosomal processing pathway for exogenous material, and (b) in outside blastomeres, the polarization of endocytotic components along the apicobasal axis of the cell. Both events proceed in a temporal sequence in outside cells with the result that three distinct phases or increments can be recognized in the generation of the trophectoderm (TE) epithelium. These stages may be defined as (a) the *apolar* condition (early cleavage up to and including the early 8-cell stage) characterized by the symmetrical organization of an immature endocytotic apparatus; (b) the *primary polarized* condition (mid 8-cell to mid 16-cell stage) in which non-lysosomal endocytotic organelles localize predominantly in the apical cytoplasm to coincide with preferential endocytotic activity from the apical membrane; and (c) the *secondary polarized* condition (late 16-cell stage onwards) characterized by the manufacture

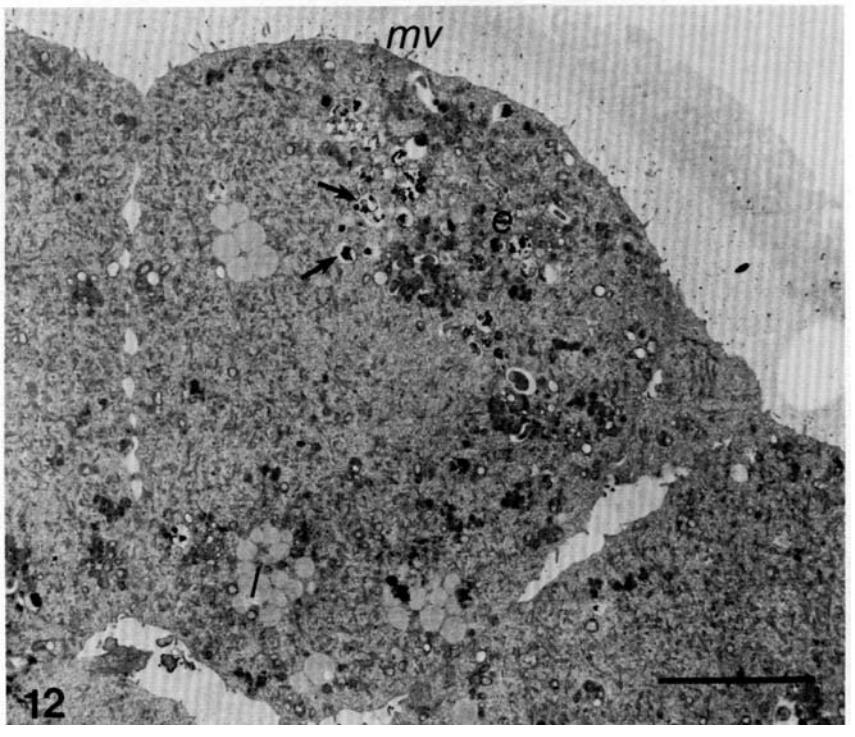

Fig. 12. Region of compacted 8-cell embryo cultured from the late 2-cell stage in M16 containing an elevated concentration of BSA (20 mg ml^{-1}). The predominant clustering of endocytotic organelles (*e*) in the apical cytoplasm is consistent with control embryos (e.g. Fig. 4B). However, the population of electron-dense degradative vacuoles (arrows) associated with endosomes is unusually large. No evidence of premature basal polarization of endocytotic organelles was obtained. *l* = lipid, *mv* = microvillous pole. Bar = 5 μm.

and basal polarization of secondary lysosomes to complete the endocytotic pathway.

The transition between phases (a) and (b) and the onset of endocytotic polarity during the 8-cell stage provides further evidence that lineage differentiation in the preimplantation embryo is a consequence of cellular events initiated at the time of compaction (Johnson, 1985*a*). The endocytotic organelles which polarize in the apical cytoplasm correspond to those described by Reeve (1981*a*) who first demonstrated the polarity of internalized HRP sites at compaction. These have been designated endosomes since they represent the primary intracellular collecting site for exogenous tracers and show no evidence of acid hydrolase activity (Helenius *et al.* 1983). Their morphology, characterized by associated tubular/vesicular structures (TVS) and, in some cases, internalized vesicles (multivesicular bodies), is also consistent with endosomal organelles described elsewhere (Helenius *et al.* 1983). It is of interest that the TVS surrounding endosomes provided little evidence of HRP labelling; this region of the complex has been shown in studies on the TE epithelium to originate from the endosome vacuole and to represent the initial stage of either recycling or transcellular pathways for internalized membrane and therefore generally do not incorporate tracers such as HRP which remain unassociated with membrane (unpublished observations).

The data on endosome distribution suggest that their apical polarization is a progressive rather than a rapid cellular event since (a) their mean concentration within the apical cytoplasm is increased at the early 16-cell stage from that at the compacted 8-cell stage (Table 1) and (b) the incidence of cells with apically polarized HRP sites (endosome pole) within cultured 2/8 or 2/16 (larger, surface polar cells) couplets increased steadily from the mid 8-cell stage (Table 3), reaching a peak at 3 h postdivision to the 16-cell stage (Table 6). An increase in the incidence of restricted HRP staining between polarized 8- and 16-cells has also been recorded by Reeve (1981*a*,*b*). This pattern is in contrast with the more synchronous appearance of surface polarity during the 8-cell stage which, although it is initiated somewhat later than endosome polarity, becomes established within the cell population relatively quickly (Table 3). Thus it is plausible that once the inductive signal to polarize is 'received' by the cell, the mechanisms involved in redistributing surface membrane and endosomal components remain distinct.

At present, the mechanism controlling surface reorganization has not been determined but recent evidence has indicated that endosome relocation is regulated by the cytoskeleton since polarization is sensitive to both cytochalasin D and colcemid treatments (Fleming *et al.* 1985). Furthermore, cytoplasmic actin (Johnson & Maro, 1984) and clathrin (Maro *et al.* 1985), a molecule intimately involved in endocytosis, have been shown to polarize apically at a similar time to endosomes, and before the appearance of surface polarity, during the 8-cell stage. Whether these represent separate events or are the manifestation of a single cytological process remains to be seen. The progressive nature of endosome polarization during the early morula period may imply a continuous process of cytoskeletal redistribution to reinforce or further stabilize the newly-established

axis of polarity. Polarized HRP sites, as well as polar actin and clathrin (Johnson & Maro, 1984; Maro *et al.* 1985), are not preserved during division to the 16-cell stage (Reeve, 1981*b*) and are evident at a reduced frequency in larger, surface polar cells immediately postdivision before their restoration to beneath the surface pole later in the cell cycle (Table 6). Since surface polarity is evident throughout the same period, it is possible that cytocortical foci direct the reassembly of a polarized internal organization, probably via cytoskeletal elements (Johnson & Maro, 1985). One route by which the cytocortex might influence cytoplasmic organization derives from the current observation that pinocytotic activity is polarized to the apical surface during the 8- and 16-cell stages in a progressive manner (compare Tables 4 and 5), thus typifying the condition found in fully differentiated epithelia (Herzog, 1984). The level of heterogeneous pinocytotic activity may therefore correlate directly with the degree of organelle polarization since it is likely to be limited by the availability of membrane recycling pathways provided by endosomes.

The second phase of endocytotic development initiated in outside cells at the late 16-cell stage is characterized by the manufacture and basal polarization of trimetaphosphatase-positive secondary lysosomes which accumulate HRP after prolonged incubation. Several organelle types including Golgi bodies and cytoplasmic granules were found to migrate to the basal zone during this period indicating that an extensive reorganization of cytoplasmic contents by the cytoskeleton has again taken place. These observations are supported by immunocytochemical evidence demonstrating a basal concentration of lysosomal and Golgi antigens at this time (Maro *et al.* 1985). Since the primary axis of cell polarity is preserved during this period of organelle redistribution, the formation and restricted localization of secondary lysosomes can be viewed as a maturation stage rather than a differentiative event in the generation of the polar cell lineage. In this context, the disposition of organelles within precursor TE cells resembles more closely the pattern observed in fully differentiated cells where Golgi elements and secondary lysosomes are positioned under the control of the cytoskeleton, along the axis of polarity (Kupfer, Dennert & Singer, 1983; Collot, Louvard & Singer, 1984).

The morphological and tracer observations indicate that basal secondary lysosomes are derived from heterogeneous processes including (a) autolytic digestion of specific cytoplasmic components (e.g. 'jigsaw' granules) and (b) endocytotic processing, probably via the transformation of endosomes according to the maturation model described by Helenius *et al.* (1983). The substructure of secondary lysosomes is comparable with that of degradative vacuoles which occur infrequently but progressively during earlier cleavage stages. However, degradative vacuoles were not found to exhibit hydrolytic activity and hence their endocytotic status (lysosomal?) cannot be classified reliably. A negative cytochemical result should be treated with caution since the correct substrate and optimal pH may not have been achieved although three techniques were applied at varying pH values. Indeed previous optical cytochemical analyses on mouse early

embryos have recorded a minimal reactivity for acid hydrolases *prior* to the 16-cell stage (Mulnard, 1965; Solter, Damjanov & Skreb, 1973), and, in an ultrastructural study, hydrolases were first detectable at a low level in the 8-cell embryo and increased thereafter up to the blastocyst stage (Vorbrodt, Konwinski, Solter & Koprowski, 1976). Thus on the basis of cytochemical data alone, we cannot infer that degradative vacuoles are entirely deficient in hydrolase enzymes and hence that the maturation and autolytic processes observed during the late 16-cell stage represent the earliest occurrence of lysosomal activity in the developing embryo. However, despite this qualification, we may at least conclude that at the morula stage there is a substantial upsurge in secondary lysosome production which also includes a qualitative change in that trimetaphosphatase activity is evident for the first time. The mobilization of Golgi elements and their association with organelles undergoing autolysis may signify the localized production of primary lysosomes. Their fusion with surrounding structures including degradative vacuoles would help to explain both the rapid onset of hydrolytic activity detected in this region of the cell and the requirement for basal polarization to congregate target organelles.

Our data are consistent with earlier studies conducted on other mammalian species (rat, rabbit) where endocytotic activity (extent of internalization of tracers) has been shown to increase progressively during cleavage (Schlafke & Enders, 1973; Hastings & Enders, 1974). Although we have interpreted the maturational changes in the mouse endocytotic system as an integral part of the process of cell polarization, and hence of tissue diversification (Johnson, 1985*b*), it is more difficult to evaluate a physiological role for these changes, other than in general terms. Biochemical data on total protein content and protein synthetic activity during mouse preimplantation development indicate a dependence on a declining store of maternal proteins for metabolic events until the early morula stage. Subsequently, there is a dramatic rise both in synthesis (six to eight fold) and in total protein by the blastocyst stage (Brinster, Wiebold & Brunner, 1976; Abreu & Brinster, 1978; Sellens, Stein & Sherman, 1981). An increase in endocytosis during cleavage, polarized to the outward facing surface of the compacted embryo and coincident with the emergence of definitive secondary lysosomes, suggests that exogenous proteins may function to a significant extent as a substrate for the recorded upsurge in synthetic activity in the late morula.

We wish to thank Dr M. H. Johnson and our research colleagues for their helpful discussions and criticisms of the manuscript. Our thanks also to Tim Crane and Roger Liles for photographic reproductions and Caroline Hunt, Anne Wright and Fiona Symington for preparing the manuscript. This work was supported by grants from the M.R.C. to Dr M. H. Johnson.

REFERENCES

Abreu, S. L. & Brinster, R. L. (1978). Synthesis of tubulin and actin during the preimplantation development of the mouse. *Expl Cell Res.* **114**, 135–141.

Bishop, O. N. (1966). *Statistics for Biology*. London: Longmans.

Borland, R. M. (1977). Transport processes in the mammalian blastocyst. In *Development in Mammals* (ed. M. H. Johnson), Vol. 1, pp. 31–67. Amsterdam, New York: North-Holland.

BRINSTER, R. L., WIEBOLD, J. L. & BRUNNER, S. (1976). Protein metabolism in preimplanted mouse ova. *Devl Biol.* **51**, 215–224.

BURGOYNE, P. S. & DUCIBELLA, T. (1977). Changes in the properties of the developing mouse trophoblast as revealed by aggregation studies. *J. Embryol. exp. Morph.* **40**, 143–157.

CALARCO, P. G. & BROWN, E. H. (1969). An ultrastructural and cytological study of preimplantation development in the mouse. *J. exp. Zool.* **171**, 253–284.

CALARCO, P. G. & EPSTEIN, C. J. (1973). Cell surface changes during preimplantation development in the mouse. *Devl Biol.* **32**, 208–213.

CHISHOLM, J. C., JOHNSON, M. H., WARREN, P. D., FLEMING, T. P. & PICKERING, S. J. (1985). Developmental variability within and between mouse expanding blastocysts and their ICMs. *J. Embryol. exp. Morph.* **86**, 311–336.

COLLOT, M., LOUVARD, D. & SINGER, S. J. (1984). Lysosomes are associated with microtubules and not with intermediate filaments in cultured fibroblasts. *Proc. natn. Acad. Sci., U.S.A.* **81**, 788–792.

DOTY, S. B., SMITH, C. E., HAND. A. R. & OLIVER, C. (1977). Inorganic trimetaphosphatase as a histochemical marker for lysosomes in light and electron microscopy. *J. Histochem. Cytochem.* **25**, 1381–1384.

DUCIBELLA, T., ALBERTINI, D. F., ANDERSON E. & BIGGERS, J. D. (1975). The preimplantation mammalian embryo: characterization of intercellular junctions and their appearance during development. *Devl Biol.* **45**, 231–250.

DUCIBELLA, T. & ANDERSON, E. (1975). Cell shape and membrane changes in the eight-cell mouse embryo: prerequisites for morphogenesis of the blastocyst. *Devl Biol.* **47**, 45–58.

DUCIBELLA, T., UKENA, T., KARNOVSKY, M. & ANDERSON, E. (1977). Changes in cell surface and cortical cytoplasmic organization during early embryogenesis in the preimplantation mouse embryo. *J. Cell Biol.* **74**, 153–167.

DUNCAN, R. & LLOYD, J. B. (1978). Pinocytosis in the rat visceral yolk sac. Effects of temperature, metabolic inhibitors and some other modifiers. *Biochim. Biophys. Acta* **544**, 647–655.

DVORAK, M. (1978). The differentiation of rat ova during cleavage. *Advances in Anatomy, Embryology and Cell Biology* 55, Fasc. 2. Springer-Verlag.

EDWARDS, R. G. & GATES, A. H. (1959). Timing of the stages of the maturation divisions, ovulation, fertilization and the first cleavage of eggs of adult mice treated with gonadotrophins. *J. Endocrinol.* **18**, 292–304.

FLEMING, T. P., CANNON, P. M. & PICKERING, S. J. (1985). The cytoskeleton, endocytosis and cell polarity in the mouse preimplantation embryo. *Devl Biol.* Submitted.

FLEMING, T. P., WARREN, P. D., CHISHOLM, J. C. & JOHNSON, M. H. (1984). Trophectodermal processes regulate the expression of totipotency within the inner cell mass of the mouse expanding blastocyst. *J. Embryol. exp. Morph.* **84**, 63–90.

FULTON, B. P. & WHITTINGHAM, D. G. (1978). Activation of mammalian oocytes by intracellular injection of calcium. *Nature* **273**, 149–151.

GOODALL, H. & JOHNSON, M. H. (1982). The use of carboxyfluorescein diacetate to study the formation of permeable channels between mouse blastomeres. *Nature* **295**, 524–526.

GOODALL, H. & JOHNSON, M. H. (1984). The nature of intercellular coupling within the preimplantation mouse embryo. *J. Embryol. exp. Morph.* **79**, 53–76.

HANDYSIDE, A. H. (1980). Distribution of antibody- and lectin-binding sites on dissociated blastomeres from mouse morulae: evidence for polarization at compaction. *J. Embryol. exp. Morph.* **60**, 99–116.

HASTINGS, R. A. & ENDERS, A. C. (1974). Uptake of exogenous protein by the preimplantation rabbit. *Anat. Rec.* **179**, 311–330.

HELENIUS, A., MELLMAN, I., WALL, D. & HUBBARD, A. (1983). Endosomes. *Trends Biochem. Sci.* **8**, 245–250.

HERZOG, V. (1984). Pathways of endocytosis in thyroid follicle cells. *Int. Rev. Cytol.* **91**, 107–139.

HOPSU-HAVA, V. K., ARSTILA, A. U., HELMINEN, H. J. & KALIMO, H. O. (1967). Improvements in the method for the electron microscopic localization of arylsulphatase activity. *Histochemie* **8**, 54–64.

IZQUIERDO, L. & EBENSPERGER, C. (1982). Cell membrane regionalization in early mouse embryos as demonstrated by 5'-nucleotidase activity. *J. Embryol. exp. Morph.* **69**, 115–126.

IZQUIERDO, L., LOPEZ, T. & MARTICORENA, P. (1980). Cell membrane regions in preimplantation mouse embryos. *J. Embryol. exp. Morph.* **59**, 89–102.

IZQUIERDO, L. & VIAL, J. D. (1962). Electron microscope observations on the early development of the rat. *Z. Zellforsch.* **56**, 157–179.

JOHNSON, M. H. (1981). Membrane events associated with the generation of a blastocyst. *Int. Rev. Cytol.* Suppl. **12**, 1–37.

JOHNSON, M. H. (1985*a*). Manipulation of early mammalian development: what does it tell us about cell lineages? In *Manipulation of Mammalian Development* (ed. R. B. L. Gwatkin). New York: Plenum Publishing Corporation.

JOHNSON, M. H. (1985*b*). Three types of cell interaction regulate the generation of cell diversity in the mouse blastocyst. In *The Cell in Contact: Adhesions and Junctions as Morphogenetic Determinants*. Neurosciences Institute Publications Series. London: John Wiley.

JOHNSON, M. H. & MARO, B. (1984). The distribution of cytoplasmic actin in mouse 8-cell blastomeres. *J. Embryol. exp. Morph.* **82**, 97–117.

JOHNSON, M. H. & MARO, B. (1985). A dissection of the mechanisms generating and stabilising polarity in mouse 8- and 16-cell blastomeres: the role of cytoskeletal elements. *J. Embryol. exp. Morph.* **90** (in press).

JOHNSON, M. H. & ZIOMEK, C. A. (1981). The foundation of two distinct cell lineages within the mouse morula. *Cell* **24**, 71–80.

JOHNSON, M. H. & ZIOMEK, C. A. (1982). Cell subpopulations in the late morula and early blastocyst of the mouse. *Devl Biol.* **91**, 431–439.

JOHNSON, M. H. & ZIOMEK, C. A. (1983). Cell interactions influence the fate of mouse blastomeres undergoing the transition from the 16- to the 32-cell stage. *Devl Biol.* **95**, 211–218.

KAYE, P. L., SCHULTZ, G. A., JOHNSON, M. H., PRATT, H. P. & CHURCH, R. B. (1982). Amino acid transport and exchange in preimplantation mouse embryos. *J. Reprod. Fert.* **65**, 367–380.

KIMBER, S. J., SURANI, M. A. H. & BARTON, S. C. (1982). Interactions of blastomeres suggest changes in cell surface adhesiveness during the formation of inner cell mass and trophectoderm in the preimplantation mouse embryo. *J. Embryol. exp. Morph.* **70**, 133–152.

KUPFER, A., DENNERT, G. & SINGER, S. J. (1983). Polarization of the Golgi apparatus and the microtubule-organizing center within cloned natural killer cells bound to their targets. *Proc. natn. Acad. Sci., U.S.A.* **80**, 7224–7228.

LEWIS, P. R. & KNIGHT, D. P. (1977). *Staining Methods for Sectioned Material.* Amsterdam-New York-Oxford: North-Holland.

LO, C. W. & GILULA, N. B. (1979). Gap junctional communication in the preimplantation mouse embryo. *Cell* **18**, 399–409.

LUFT, J. H. (1971). Ruthenium red and violet. II. Fine structural localization in animal tissues. *Anat. Rec.* **171**, 369–416.

MAGNUSON, T., DEMSEY, A. & STACKPOLE, C. W. (1977). Characterization of intercellular junctions in the preimplantation mouse embryo by freeze-fracture and thin-section electron microscopy. *Devl Biol.* **61**, 252–261.

MARO, B., JOHNSON, M. H., PICKERING, S. J. & LOUVARD, D. (1985). Changes in the distribution of membraneous organelles during mouse early development. *J. Embryol. exp. Morph.* **90** (in press).

MCLACHLIN, J. R., CAVENEY, S. & KIDDER, G. M. (1983). Control of gap junction formation in early mouse embryos. *Devl Biol.* **98**, 155–164.

MULNARD, J. G. (1965). Studies of regulation of mouse ova *in vitro*. In *Preimplantation Stages of Pregnancy* (ed. G. E. W. Wolstenholme & M. O'Connor), Ciba Foundation Symposium, pp. 123–138. London: Churchill.

MULNARD, J. & HUYGENS, R. (1978). Ultrastructural localization of non-specific alkaline phosphatase during cleavage and blastocyst formation in the mouse. *J. Embryol. exp. Morph.* **44**, 121–131.

NADIJCKA, M. & HILLMAN, N. (1974). Ultrastructural studies of the mouse blastocyst substages. *J. Embryol. exp. Morph.* **32**, 675–695.

NICOLSON, G. L., YANAGIMACHI, R. & YANAGIMACHI, H. (1975). Ultrastructural localization of lectin-binding sites on the zonae pellucidae and plasma membranes of mammalian eggs. *J. Cell Biol.* **66**, 263–274.

PRATT, H. P. M. (1985). Membrane organization in the preimplantation mouse embryo. *J. Embryol. exp. Morph.* **90** (in press).

RANDLE, B. J. (1982). Cosegregation of monoclonal antibody reactivity and cell behaviour in the mouse preimplantation embryo. *J. Embryol. exp. Morph.* **70**, 261–278.

REEVE, W. J. D. (1981*a*). Cytoplasmic polarity develops at compaction in rat and mouse embryos. *J. Embryol. exp. Morph.* **62**, 351–367.

REEVE, W. J. D. (1981*b*). The distribution of ingested horseradish peroxidase in the 16-cell mouse embryo. *J. Embryol. exp. Morph.* **66**, 191–207.

REEVE, W. J. D. & KELLY, F. P. (1983). Nuclear position in the cells of the mouse early embryo. *J. Embryol. exp. Morph.* **75**, 117–139.

REEVE, W. J. D. & ZIOMEK, C. A. (1981). Distribution of microvilli on dissociated blastomeres from mouse embryos: evidence for surface polarization at compaction. *J. Embryol. exp. Morph.* **62**, 339–350.

REGGIO, H., COUDRIER, E. & LOUVARD, D. (1982). Surface and cytoplasmic domains in polarised epithelial cells. In *Membranes in Growth and Development.* pp. 89–105. New York: Alan R. Liss.

RINDLER, M. J., IVANOV, I. E., RODRIGUEZ-BOULAN, E. J. & SABATINI, D. D. (1982). Biogenesis of epithelial cell plasma membranes. In *Membrane Recycling.* Ciba Foundation Symposium 92, pp. 184–202. London: Pitman.

RODEWALD, R. & ABRAHAMSON, D. R. (1982). Receptor-mediated transport of IgG across the intestinal epithelium of the neonatal rat. In *Membrane Recycling.* Ciba Foundation Symposium 92, pp. 209–226. London: Pitman.

SABATINI, D. D., GRIEPP, E. B., RODRIGUEZ-BOULAN, E. J., DOLAN, W. J., ROBBINS, E. S., PAPADOPOULOS, S., IVANOV, I. E. & RINDLER, M. J. (1983). Biogenesis of epithelial cell polarity. In *Modern Cell Biology* Vol. 2, pp. 419–450. New York: Alan R. Liss.

SCHLAFKE, S. & ENDERS, A. C. (1967). Cytological changes during cleavage and blastocyst formation in the rat. *J. Anat.* **102**, 13–32.

SCHLAFKE, S. & ENDERS, A. C. (1973). Protein uptake by rat preimplantation stages. *Anat. Rec.* **175**, 539–560.

SEARLE, R. F. & JENKINSON, E. J. (1978). Localization of trophoblast-defined surface antigens during early mouse embryogenesis. *J. Embryol. exp. Morph.* **43**, 147–156.

SELLENS, M. H., STEIN, S. & SHERMAN, M.I. (1981). Protein and free amino acid content in preimplantation mouse embryos and in blastocysts under various culture conditions. *J. Reprod. Fert.* **61**, 307–315.

SOLTER, D. DAMJANOV, I. & SKREB, N. (1973). Distribution of hydrolytic enzymes in early rat and mouse embryos: a reappraisal. *Z. Anat. EntwGesch.* **139**, 119–126.

SOTELO, J. R. & PORTER, K. R. (1959). An electron microscope study of the rat ovum. *J. Biophys. Biochem. Cytol.* **5**, 327–342.

STASTNA, J. (1974). Origin and function of multivescular bodies in the segmenting ovum of rat. *Acta Fac. Med. Univ. Brun.* **49**, 87–98.

VOBRODT, A., KONWINSKI, M., SOLTER, D. & KOPROWSKI, H. (1976). Ultrastructural localization of cytoplasmic phosphatases in preimplantation mouse embryos. *Folia Histochem. Cytochem.* **14**, 249–256.

WHITTINGHAM, D. G. (1971). Culture of mouse ova. *J. Reprod. Fert. (Suppl.)* **14**, 7–21.

WILEY, L. M. & EGLITIS, M. A. (1981). Cell surface and cytoskeletal elements: cavitation in the mouse preimplantation embryo. *Devl Biol.* **86**, 493–501.

ZIOMEK, C. A. & JOHNSON, M. H. (1981). Properties of polar and apolar cells from the 16-cell mouse morula. *W. Roux' Arch. devl Biol.* **190**, 287–296.

ZIOMEK, C. A. & JOHNSON, M. H. (1982). The roles of phenotype and position in guiding the fate of 16-cell mouse blastomeres. *Devl Biol.* **91**, 440–447.

ZIOMEK, C. A., JOHNSON, M. H. & HANDYSIDE, A. H. (1982). The developmental potential of mouse 16-cell blastomeres. *J. exp. Zool.* **221**, 345–355.

(Accepted 14 March 1985)